Polar Sampler: Discrete Gaussian Sampling over the Integers Using Polar Codes

Jiabo Wang, Cong Ling, *Member, IEEE*

Abstract

Cryptographic constructions based on hard lattice problems have emerged as a front runner for the standardization of post quantum public key cryptography. As the standardization process takes place, optimizing specific parts of proposed schemes becomes a worthwhile endeavor. Gaussian sampling over the integers is one of the fundamental building blocks of latticed-based cryptography. In this work, we propose a new integer Gaussian sampler based on polar codes, dubbed "polar sampler". The polar sampler is asymptotically information theoretically optimum in the sense that the number of uniformly random bits it uses approaches the entropy bound. It also features quasi-linear complexity and constant-time implementation. Our algorithm becomes effective when sufficiently many samples are required at each query to the sampler. Security analysis is given based on the statistical distance, Kullback-Leibler divergence and Rényi divergence. A comparison between the polar sampler and the Knuth-Yao sampler verifies its time efficiency and the memory cost can be further optimized if space-efficient successive-cancellation decoding is adopted.

Index Terms

Discrete Gaussian sampling, polar codes, integer lattice, Kullback-Leibler divergence, constant-time implementation.

I. Introduction

Lattice-based cryptography is one of the most promising candidates of cryptosystems in the future post-quantum age. The security of lattice-based primitives is guaranteed by the hardness of worst-case lattice problems, e.g. the Learning With Errors (LWE) problem [1], [2] and Short Integer Solution (SIS) problem [3], [4]. The discrete Gaussian distribution lies at the core of security proofs of these

This work was supported in part by the China Scholarship Council and EPSRC.

J. Wang and C. Ling are with the Department of Electrical and Electronic Engineering, Imperial College London, London SW7 2AZ, U.K. (e-mail: j.wang16@imperial.ac.uk; cling@ieee.org).

primitives, and it is also one of the fundamental building blocks of practical lattice-based cryptographic applications, e.g. signature schemes, encryption and key exchanges. In general, the security level of these cryptographic applications is closely related to the statistical performance of the discrete Gaussian sampling (DGS) algorithm. From an implementation standpoint, cryptographers also take other qualities of a DGS into consideration including side-channel resistance, computation and storage efficiency. In practice, the tradeoff between these performances is a bottleneck of this problem.

It has been widely assumed that for cryptographic applications with λ bits of security the statistical distance (SD) between the ideal distribution and the approximated one should be roughly $2^{-\lambda}$ such that there is only minor loss in security [5]. Some other measures such as Kullback-Leibler (KL) divergence and Rényi divergence are proved to provide more efficient security analysis than the SD, as they can lower the requirement for precision and reduce the cost of the algorithms in many practical cases [6], [7], [8], [9]. From a practical point of view, the difficulty of DGS lies in the implementation of DGS in cryptographic primitives with constrained resources. Besides the resilience against potential side-channel attacks, a designer looking for the optimal DGS solution to a specific application strikes the balance of memory consumption and running time, precision and efficiency.

There are already a variety of works addressing the application of DGS in lattice-based primitives. Existing techniques include the Bernoulli sampler [10], the cumulative distribution table (CDT) sampler [11], the Knuth-Yao sampler [12], and the discrete Ziggurat sampler [13], etc. Rejection sampling can be used to generate discrete Gaussian samples where one draws an element x from a discrete domain uniformly at random and accepts it with probability proportional to $\exp(-x^2/2\sigma^2)$ where σ is the standard deviation. However, calculating the exponential function requires high-precision computing and sufficient trials are needed before the sampler produces an output. In [14], Peikert suggested to perform binary search through CDT and he adapted it to the signature scheme BLISS [10]. At the first step of BLISS, a discrete Gaussian vector is generated to blind the secret. However, the CDT sampling itself takes 35 percent of the total running time of BLISS [15] and the precomputed CDT requires larger memory especially when a wider distribution is in need to improve the security level.

In [16], Hülsing et al. replaced the discrete Gaussian distribution in Lyubashevsky's signature scheme and BLISS by a rounded Gaussian distribution and proved that these schemes were safe. As the term suggested, a rounded Gaussian distribution is obtained by rounding continuous Gaussian samples which can be efficiently realized by Box-Muller transform [17] in constant time. A convolution method, first proposed in [14], can expand a discrete Gaussian distribution with a small parameter to a wider one. A recent sampler design [18] exploits a base sampler with small parameters to efficiently generate DGS with arbitrary and varying parameters in a convolutional fashion. This application-independent algorithm

consists of an online and offline stage, both of which can be carried out in constant time, proving a resilience against timing attack. [19] proposed a constant-time sampler and applied Rényi divergence analysis to their algorithm. [20] proposed a DGS algorithm for lattice signatures using arithmetic coding.

A. Contribution

In this work, we propose a novel algorithm for DGS over the integers using polar codes. Polar codes are the first class of efficiently encodable and decodable codes which provably achieve Shannon's entropy bound in source coding and channel capacity in channel coding, respectively [21], [22]. The power of polar codes stems from the polarization phenomenon: under Arikan's polar transform, information measures of synthesized sources (channels) converge to either 0 or 1 when coding becomes trivial. Moreover, both encoding and decoding run with $O(N \log N)$ complexity, where N denotes the length of a polar code. Given their attractive performance, polar codes have found a wide range of applications in information theory and communication systems. In particular, they have been standardized for the upcoming fifth-generation (5G) wireless communication networks.

This work tackles the sampling problem from a source coding perspective, namely, sampling can be considered the inverse problem of source coding. In source coding or data compression, one typically encode a block of symbols of a certain distribution into some bits which become uniformly random as the block-length tends to infinity [23]. Since a source code is invertible, inverting this process would produce samples from the desired distribution. When a large number of independent Gaussian samples are required in cryptographic applications, polar codes are well suited because in this case the information source of distribution $D_{\mathbb{Z}^N,c,s}$ is memoryless. Obviously, this technique is not restricted to sampling from the discrete Gaussian distribution, but can be extended to other distributions of interest in cryptography.

The principal contributions of this paper are summarized as follows:

- A novel approach to sample from discrete Gaussian distribution over the integers with multilevel polar codes. Using a binary partition tree, we recursively partition $\mathbb{Z}$ into 2 cosets, 4 cosets, and so on. The number of levels is only logarithmic in s. Each level gives rise to a binary source, which is compressed by a binary polar code. The advantage of this multilevel coding approach is that only binary codes are needed, which allow simpler implementation than nonbinary codes.
- Analysis of approximation errors. Although inverting this multilevel polar code would produce the desired distribution $D_{\mathbb{Z}^N,c,s}$, it is not exactly so. This is because the bits after compression are not exactly uniformly random, so feeding the inverted source code with uniformly random bits will only yield an approximate version of the desired distribution. We derive upper bounds on the closeness of the target discrete Gaussian and its approximation by our polar sampler, in SD and KL divergence.

- Security analysis. To achieve a certain security level in a standard cryptographic scheme with oracle access to a discrete Gaussian distribution, the principle of setting the parameters of our polar sampler is also discussed. In cryptographic applications where the number of queries q to the Gaussian sampler is limited (e.g., $q \leq 2^{64}$ in the NIST specifications of signatures), it is well known that using Rényi divergence yields considerable savings. We also apply Rényi divergence to analyse the security level associated with the proposed polar sampler.

The proposed polar sampler complements and distinguishes from existing discrete Gaussian samplers in the literature. In addition to offering a different approach, it exhibits several salient features:

- Information theoretic optimality. Asymptotically, the polar sampler achieves the entropy bound of the discrete Gaussian distribution. This implies that it requires minimum resources of random bits to produce the desired distribution.
- Quasi-linear complexity. The multilevel approach to Gaussian sampling enjoys low complexity. Both design and implementation require quasi-linear complexity $O(N \log N)$ in storage and running time. The design can be done at the offline stage, that is, given a target distribution, it is done once and for all. The online stage of implementation requires certain a posteriori probabilities, which can be computed in a successive manner. The polar transform itself can be implemented efficiently in $O(N \log N)$ complexity.
- Constant-time implementation. The polar sampler also admits constant-time implementation, since a polar code has a fixed-length. This compares favorably with other source coding techniques such as Huffman coding whose codewords have variable lengths. Moreover, all the computations required run in constant time. This makes our polar sampler very attractive when dealing with side-channel (e.g., timing) attacks.

Of course, the proposed sampler can be combined with existing "expander" techniques such as convolution if needed. In this paper, we focus on the theoretic design and analysis of polar samplers, whereas various optimization issues (e.g., concrete computational/storage costs, finite precision etc.) are left to future work. Nevertheless, we have found it in experiments that even a prototype implementation significantly outperforms benchmark Knuth-Yao sampling in speed.

The polarization transform separates the unpredictable content of a source from its predictable part. This resembles the terminology "extractor" in theoretical computer science which can also achieve information theoretic optimality but in a distinct manner. Normally, extractors aim at the min-entropy of a family of distributions rather than the Shannon's entropy of an i.i.d. source from a known distribution. For example, the Toeplitz-hashing based extractor is able to extract the min-entropy of a source by multiplying the raw

data by a Toeplitz matrix with quasilinear complexity, but it requires an extra seed at the input. Therefore it is not information theoretically optimal in the context of discrete Gaussian sampling.

B. Roadmap

The roadmap of this paper is given as follows. Section II introduces the preliminaries of polar source coding and elucidates its relation to sampling. Section III presents our polar sampler in detail. Section IV gives an analysis on the approximation error of our sampler based on both SD and KL divergence. In Section V, the security level of our sampler is analysed based on SD and KL divergence, respectively. Section VI compares the polar sampler with Knuth-Yao and Micciancio and Walter's sampler [18] regarding the complexity. Section VII concludes this paper and gives some suggestions on future work.

II. Source Coding versus Sampling

A. Notation

We use the notation $x^{1:N}$ as shorthand for a row vector $(x^{(1)}, \cdots, x^{(N)})$ of which the i-th entry is denoted by $x^{(i)}$. Given a vector $x^{1:N}$ and a set $\mathcal{A} \subset \{1, \cdots, N\}$, $x_{\mathcal{A}}$ denotes the subvector of $x^{1:N}$ indexed by $\mathcal{A}$. Capital letters such as U and X are used to denote variables while lowercase letters such as u and x represent a realization of the corresponding variable. Denote by $X \sim P$ a distribution P of X over a countable set $\mathcal{X}$. Then the entropy of X is defined as $H_P(X) = -\sum_{x\in\mathcal{X}} p(x) \log p(x)$. We write $H(X) = H_P(X)$ for brevity if the distribution is clear. Suppose X and Y have a joint distribution $P(X, Y)$. The conditional entropy of X given Y is defined as $H(X|Y) = \sum_{x\in\mathcal{X}, y\in\mathcal{Y}} p(x, y) \log \frac{p(y)}{p(x,y)}$. The logarithm to base 2 is denoted by $\log$ while the natural logarithm is denoted by $\ln$.

B. Source Polarization

The key idea of polar source coding can be found in [22] where a polar code was proposed to achieve Shannon's source coding bound. Let $(X^{1:N}, Y^{1:N})$ denotes N i.i.d. copies of a memoryless source $(X, Y) \sim P_{X,Y}$, where X takes values over $\mathcal{X} = \{0, 1\}$ while Y takes values over a countable set $\mathcal{Y}$. The two random source X and Y are correlated, and Y is called the side-information[1]. In source coding, the encoder compresses a sequence $X^{1:N}$ into a shorter codeword, such that the decoder can produce an estimation $\hat{X}^{1:N}$ of $X^{1:N}$ using the codeword side information $Y^{1:N}$.

[1]Note that even if there is only one source in the context of this paper, the proposed multilevel code still needs side information (which is basically information coming from lower levels.)

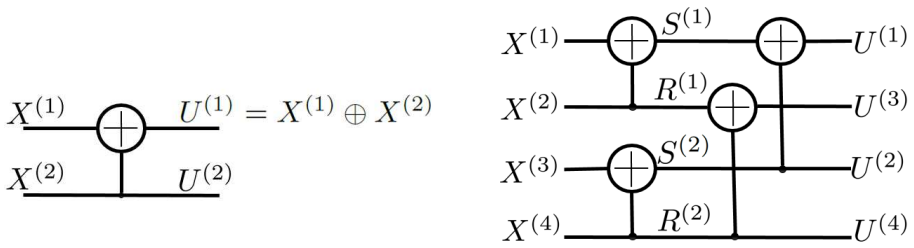

(a) (b)

Fig. 1. The source polarization transform [21]: (a) A two-by-two transform (b) A four-by-four transform.

Polar codes are proved to achieve Shannon's source coding bound asymptotically. The source polarization transform from $X^{1:N}$ to $U^{1:N}$ is performed by applying an entropy-preserving circuit to $X^{1:N}$, i.e.,

$$U^{1:N} = X^{1:N} G_N$$

and

$$G_N = \begin{bmatrix} 1 & 1 \\ 1 & 0 \end{bmatrix}^{\otimes n} B_N,$$

where $^{\otimes n}$ denotes the n-th Kronecker power, and B_N is a bit-reversal permutation [21] of the input vector. Fig. 1 illustrates the source polarization transforms of $X^{1:2}$ and $X^{1:4}$ where $\oplus$ denotes mod-2 sum. This transform preserves the entropy in the sense that

$$H(U^{1:2} \mid Y^{1:2}) = 2H(X \mid Y), \;\; H(U^{1:4} \mid Y^{1:4}) = 4H(X \mid Y).$$

Meanwhile, it also polarizes the entropy in the sense that

$$H(U^{(1)} \mid Y^{1:4}) \geq H(S^{(1)} \mid Y^{1:2}) = H(S^{(2)} \mid Y^{3:4}) \geq H(U^{(2)} \mid Y^{1:4}, U^{(1)}),$$

and

$$\begin{aligned} H(U^{(3)} \mid Y^{1:4}, U^{1:2}) \geq & H(R^{(1)} \mid Y^{1:2}, S^{(1)}) \\ = & H(R^{(2)} \mid Y^{3:4}, S^{(2)}) \geq H(U^{(4)} \mid Y^{1:4}, U^{1:3}). \end{aligned}$$

By applying the construction in Fig. 1 recursively, we can obtain the induced joint distribution of $(U^{1:N}, Y^{1:N})$ as

$$\begin{aligned} P_{U^{1:N},Y^{1:N}} &= \sum_{x^{1:N}} P_{X^{1:N},Y^{1:N}}(x^{1:N}, y^{1:N}) \cdot \mathbb{I}\{u^{1:N} = x^{1:N} G_N\} \\ &= \sum_{x^{1:N}} \left(\prod_{i=1}^{N} P_{X,Y}(x^{(i)}, y^{(i)}) \right) \cdot \mathbb{I}\{u^{1:N} = x^{1:N} G_N\}, \end{aligned} \tag{1}$$

where $\mathbb{I}\{\cdot\}$ is the indicator function. By computing the conditional entropy $H(U^{(i)} \mid Y^{1:N}, U^{1:i-1})$, we have the following source polarization theorem.

Theorem 1 (Source Polarization [22]): Let (X, Y) be a source as above. For any $N = 2^n$,$n \geq 1$, let $U^{1:N} = X^{1:N}G_N$. Then, for any $0 < \beta < 0.5$, as $N \to \infty$,

$$\frac{\left|\left\{i \in [1, N] : H(U^{(i)} \mid Y^{1:N}, U^{1:i-1}) \in (1 - 2^{-N^\beta}, 1]\right\}\right|}{N} \to H(X \mid Y) \tag{2}$$

and

$$\frac{\left|\left\{i \in [1, N] : H(U^{(i)} \mid Y^{1:N}, U^{1:i-1}) \in [0, 2^{-N^\beta})\right\}\right|}{N} \to 1 - H(X \mid Y). \tag{3}$$

Note that in the absence of side information Y, the above theorem still holds by considering Y independent of X.

Definition 1 (Bhattacharyya Parameter [24]): Let $(X, Y) \in \mathcal{X} \times \mathcal{Y}$ be a pair of random variables where $\mathcal{X} = \{0, 1\} =$ GF(2) and $\mathcal{Y}$ is an arbitrary finite set. Let X and Y follow the joint distribution $P_{XY}(x, y)$. If X is the source to be compressed and Y is the side information, the Bhattacharyya parameter is defined as

$$\begin{aligned} Z(X|Y) &\equiv 2\sum_y P_Y(y)\sqrt{P_{X|Y}(0|y)P_{X|Y}(1|y)} \\ &= 2\sum_y \sqrt{P_{X,Y}(0, y)P_{X,Y}(1, y)}. \end{aligned} \tag{4}$$

Proposition 1 ([22], Proposition 2):

$$(Z(X|Y))^2 \leq H(X|Y) \tag{5}$$

$$H(X|Y) \leq \log(1 + Z(X|Y)). \tag{6}$$

It is implied by Proposition 1 that for a source (X, Y), the parameters $H(U^{(i)} \mid Y^{1:N}, U^{1:i-1})$ and $Z(U^{(i)} \mid Y^{1:N}, U^{1:i-1})$ polarize simultaneously in the sense that $H(U^{(i)} \mid Y^{1:N}, U^{1:i-1})$ approaches 0 (resp. 1) as $Z(U^{(i)} \mid Y^{1:N}, U^{1:i-1})$ approaches 0 (resp. 1).

For $\beta \in (0, 1/2)$ and $\alpha = 2^{-N^\beta}$, the indexes of $U^{1:N}$ can be divided into a low-entropy set

$$\mathcal{L}_{X|Y} = \left\{i \in [N] : \ Z(U^{(i)} \mid Y^{1:N}, U^{1:i-1}) \in [0, \alpha)\right\} \tag{7}$$

and its complement ${\mathcal{L}^c}_{X|Y}$. Again, in the absence of side information Y, the two sets are defined in the same way by considering Y independent of X and U.

This gives rise to the encoding and decoding scheme described in [22]. More specifically, for a realization of $(X^{1:N}, Y^{1:N}) = (x^{1:N}, y^{1:N})$, the encoder computes $u^{1:N} = x^{1:N}G_N$ and only shares

$u_{\mathcal{L}^c_{X|Y}}$ with the decoder. The compression rate is defined as $R = |\mathcal{L}^c_{X|Y}|/N$. The decoder can obtain an estimate $\hat{u}^{1:N}$ of $u^{1:N}$ in a successive manner as

$$\hat{u}^{(i)} = \begin{cases} u^{(i)}, & \text{if } \ i \in \mathcal{L}^c_{X|Y} \\ 0, & \text{if } \ i \in \mathcal{L}_{X|Y} \text{ and } L_N^{(i)}(y^{1:N}, \hat{u}^{1:i-1}) \geq 1 \\ 1, & \text{if } \ i \in \mathcal{L}_{X|Y} \text{ and } L_N^{(i)}(y^{1:N}, \hat{u}^{1:i-1}) < 1, \end{cases} \tag{8}$$

where $L_N^{(i)}(y^{1:N}, \hat{u}^{1:i-1})$ is called the likelihood ratio (LR) defined by

$$L_N^{(i)}(y^{1:N}, \hat{u}^{1:i-1}) = \frac{P(U^{(i)} = 0 | Y^{1:N} = y^{1:N}, U^{1:i-1} = \hat{u}^{1:i-1})}{P(U^{(i)} = 1 | Y^{1:N} = y^{1:N}, U^{1:i-1} = \hat{u}^{1:i-1})}. \tag{9}$$

The probability of block error measured by $P_e = \Pr(\hat{U}^{1:N} \neq U^{1:N}) = \Pr(\hat{U}_{\mathcal{L}_{X|Y}} \neq U_{\mathcal{L}_{X|Y}})$ is upper-bounded by

$$P_e \leq \sum_{i \in \mathcal{L}_{X|Y}} Z(U^{(i)} | Y^{1:N}, U^{1:i-1}), \tag{10}$$

which can be further formalized as a theorem as follows.

Theorem 2 (An upper bound on error probability [22]): For any fixed $R > H(X|Y)$ and $\beta < 0.5$, the probability of error for the above polar source coding method is bounded as $P_e = O(2^{-N^\beta})$.

It implies that any rate $R > H(X|Y)$ is achievable with a vanishing block error probability for sufficiently large N. As N goes to infinity, the polarization process removes the randomness of the low-entropy set almost surely while the other set becomes random. Additionally, the complexity of polar encoding and decoding are both $O(N \log N)$. More details on the complexity of successive-cancellation (SC) decoding can be found in Appendix A.

C. From Source Coding to Sampling

Now consider the sampling problem. To produce the above memoryless source X given side information Y, we further define a high-entropy set[2]

$$\mathcal{H}_{X|Y} = \left\{ i \in [N] : \ Z(U^{(i)} \mid Y^{1:N}, U^{1:i-1}) \in (1-\alpha, 1] \right\}. \tag{11}$$

According to polar source coding, the $U^{(i)}$ for $i \in \mathcal{H}_{X|Y}$ with very high entropy is approximately uniformly distributed and is approximately independent of both $U^{1:i-1}$ and the side information $Y^{1:N}$, while the $U^{(i)}$ for $i \in \mathcal{L}_{X|Y}$ with very low entropy is almost deterministic. Those $U^{(i)}$ for $i \in \mathcal{H}^c_{X|Y} \backslash \mathcal{L}_{X|Y}$ (i.e., $Z(U^{(i)} \mid Y^{1:N}, U^{1:i-1}) \in [\alpha, 1-\alpha]$) are unpolarized. As N goes to infinity, the fraction of

[2]In [22], $\mathcal{L}^c{}_{X|Y}$ is called the high-entropy set, which is larger than $\mathcal{H}_{X|Y}$.

unpolarized indexes vanishes and the fraction of high-entropy indexes approaches the entropy of X given Y according to Theorem 1.

Since the polarization transform is reversible, it is expected to produce an approximation $Q_{X^{1:N}}$ of $P_{X^{1:N}}$ by applying the above transform to $U^{1:N}$, i.e. $X^{1:N} = G_N U^{1:N}$. However, the unpolarized set may not be negligible for finite length N, and should be handled with care. More precisely, those $U^{(i)}$ for $i \in \mathcal{H}^c_{X|Y} \backslash \mathcal{L}_{X|Y}$ are not quite uniform; feeding them with uniform bits may cause non-negligible distortion from the target distribution. Therefore, for sampling, $U^{(i)}$s should follow the distribution:

$$U^{(i)} = \begin{cases} \{0,1\} \sim \text{Bernoulli}(0.5), & \text{if } i \in \mathcal{H}_{X|Y} \\ \arg\max_u P_{U^{(i)}|Y^{1:N},U^{1:i-1}}(u|y^{1:N}, u^{1:i-1}), & \text{if } i \in \mathcal{L}_{X|Y} \end{cases} \tag{12}$$

and

$$U^{(i)} = \begin{cases} 0 \quad w.p. \ P_{U^{(i)}|Y^{1:N},U^{1:i-1}}(0|y^{1:N}, u^{1:i-1}) \\ 1 \quad w.p. \ P_{U^{(i)}|Y^{1:N},U^{1:i-1}}(1|y^{1:N}, u^{1:i-1}) \end{cases} \text{if } i \in \mathcal{H}^c_{X|Y} \backslash \mathcal{L}_{X|Y} \quad . \tag{13}$$

Fig. 2 shows the difference between source coding and sampling: although the unpolarized set belongs to the compressed codeword in source coding, its bits should be randomized as in (13) in sampling. Denote

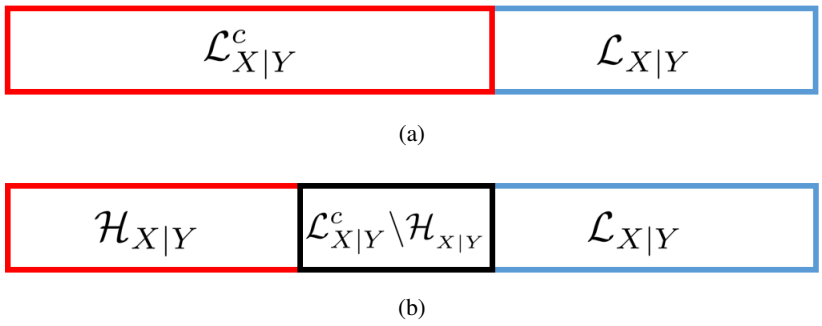

Fig. 2. Polar source coding vs. polar sampling: (a) Subsets of indexes for polar source coding (b) Subsets of indexes for polar sampling. The fraction of $\mathcal{L}^c_{X|Y} \backslash \mathcal{H}_{X|Y}$ vanishes as N goes to infinity.

by $P_{U^{1:N}}$ (resp. $Q_{U^{1:N}}$) the distribution of $U^{1:N}$ (resp. $U^{1:N}$) induced by the polarization transform, see (1). For some useful metric δ, the distance between $P_{X^{1:N}}$ and $Q_{X^{1:N}}$ is bounded by the data processing inequality

$$\delta(P_{X^{1:N}}, Q_{X^{1:N}}) \leq \delta(P_{U^{1:N}}, Q_{U^{1:N}}).$$

The goodness of a metric sometimes can help reduce the complexity of implementation. To evaluate the performance of our sampling scheme, we will compare different metrics in the sequel, e.g. SD, KL divergence and Rényi divergence.

In order to carry out the operations given in (12) and (13), one needs to compute $P_{U^{(i)}|Y^{1:N},U^{1:i-1}}$ and define the two sets $\mathcal{H}_{X|Y}$ and $\mathcal{L}_{X|Y}$ based on the Bhattacharyya parameter $Z(U^{(i)} \mid Y^{1:N}, U^{1:i-1})$. To calculate $Z(U^{(i)} \mid Y^{1:N}, U^{1:i-1})$ efficiently we can formulate (X, Y) into a binary memoryless symmetric source pair. Denote by W a transition from X to Y with probability $W(y|x) = P_{X,Y}(X, Y)/P_X(x)$. A source pair (X, Y) given as above is said to be symmetric if there exists a permutation $\pi(\cdot)$ such that $W(y|0) = W(\pi(y)|1)$. Some efficient algorithms to calculate the Bhattacharyya parameters for symmetric source pairs were proposed in [25], [26]. Meanwhile, $P_{U^{(i)}|Y^{1:N},U^{1:i-1}}$ can be computed with quasi-linear complexity by SC decoding proposed in [21].

[24, Theorem 2] originally gives the connection between the Bhattacharyya parameters of an asymmetric channel and a symmetric one and we restate it as Theorem 3 to fit in our setting. From a high level, $Z(U^{(i)} \mid Y^{1:N}, U^{1:i-1})$ can be equivalently obtained by calculating the Bhattacharyya parameters of the symmetrized version of the source pair (X, Y).

Theorem 3 (Connection Between Bhattacharyya Parameters, adapted from [24], [27]): Denote by (X, Y) a source pair with a joint distribution $P_{X,Y}$ where $X \in \mathcal{X} = \{0, 1\}$ and $Y \in \mathcal{Y}$ for some countable set $\mathcal{Y}$. Let $\tilde{X}$ takes values over $\mathcal{X}$ uniformly and let $\tilde{Y} = (\tilde{X} \oplus X, Y)$. $\tilde{X}$ and $\tilde{Y}$ can naturally be regarded as a BMS source pair with transition probability $\tilde{W}(\tilde{y}|\tilde{x}) = P_{X,Y}(x, y)$ where $\tilde{X} \in \mathcal{X}$ and $\tilde{Y} \in \tilde{\mathcal{Y}} = \mathcal{X} \times \mathcal{Y}$. By performing the above transformation circuit G_N to N i.i.d. copies of X and $\tilde{X}$, i.e., $U^{1:N} = X^{1:N}G_N$ and $\tilde{U}^{1:N} = \tilde{X}^{1:N}G_N$, respectively, we can have two combined transition blocks $W_N : U^{1:N} \to Y^{1:N}$ and $\tilde{W}_N : \tilde{U}^{1:N} \to \tilde{Y}^{1:N}$, respectively. These two combined transitions can be split back into a set of N sub-source pairs $(U^{(i)}, Y^{1:N} \times U^{1:i-1})$ giving rise to N sub-transitions $W_N^{(i)} : \mathcal{X} \to \mathcal{Y}^{1:N} \times \mathcal{X}^{1:i-1}$ and $\tilde{W}_N^{(i)} : \mathcal{X} \to \tilde{\mathcal{Y}}^{1:N} \times \mathcal{X}^{1:i-1}$, respectively. For each sub-transition of W_N and $\tilde{W}_N$, we have the following properties regarding the probability distribution and the Bhattacharyya parameter, i.e.,

$$P_{U^{1:i},Y^{1:N}}(u^{1:i}, y^{1:N}) = 2^{N-1} P_{\tilde{U}^{1:i-1},\tilde{Y}^{1:N}|\tilde{U}^{(i)}}(u^{1:i-1}, (0, y^{1:N})|u^{(i)}), \tag{14}$$

and

$$Z(U^{(i)}|U^{1:i-1}, Y^{1:N}) = \tilde{Z}(\tilde{U}^{(i)}|\tilde{U}^{1:i-1}, X^{1:N} \oplus \tilde{X}^{1:N}, Y^{1:N}). \tag{15}$$

It is straightforward to see that the Bhattacharyya parameter of the symmetric source pair and asymmetric source pair are the same, and one can calculate $\tilde{Z}(\tilde{U}^{(i)}|\tilde{U}^{1:i-1}, X^{1:N} \oplus \tilde{X}^{1:N}, Y^{1:N})$ with the known

technique for symmetric polar codes [25], [26]. Furthermore, we can have

$$\frac{P_{U^{1:i},Y^{1:N}}(u^{1:i-1},0,y^{1:N})}{P_{U^{1:i},Y^{1:N}}(u^{1:i-1},1,y^{1:N})} = \frac{P_{U^{(i)}|Y^{1:N},U^{1:i-1}}(0|y^{1:N},u^{1:i-1})}{P_{U^{(i)}|Y^{1:N},U^{1:i-1}}(1|y^{1:N},u^{1:i-1})} \tag{16}$$

$$= \frac{P_{\tilde{U}^{1:i-1},\tilde{Y}^{1:N}|\tilde{U}^{(i)}}(\tilde{u}^{1:i-1},(0^{1:N},y^{1:N})|0)}{P_{\tilde{U}^{1:i-1},\tilde{Y}^{1:N}|\tilde{U}^{(i)}}(\tilde{u}^{1:i-1},(0^{1:N},y^{1:N})|1)} \tag{17}$$

$$= L_N^{(i)}((0^{1:N},y_1^N),\tilde{u}^{1:i-1}), \tag{18}$$

where $L_N^{(i)}((0^{1:N},y_1^N),\tilde{u}^{1:i-1})$ denotes the a posterior probability ratio for a sub-transition $\tilde{W}_N^{(i)}$. Therefore, the posterior probability $P_{U^{(i)}|Y^{1:N},U^{1:i-1}}$ in (12) and (13) can be equivalently computed with complexity $O(N\log N)$ by the SC decoding proposed in [21][3]. In the same fashion, we can compute $P_{U^{(i)}|U^{1:i-1}}$ by considering Y independent of X.

III. Polar Sampling over the Integers

Definition 2: For any vectors c, x and any $s > 0$, let

$$\rho_{c,s}(x) = \exp(-\pi\|x-c\|^2/s^2)$$

be a Gaussian function on $\mathbb{R}$ centred at $x = c$ with parameter s. The total mass of the function is $\int_{x\in\mathbb{R}} \rho_{\mathbf{c},s}(x)dx = s$.

Definition 3: For any $c \in \mathbb{R}$, $s > 0$, define the discrete Gaussian distribution over $\mathbb{Z}$ as

$$\forall x \in \mathbb{Z},\ D_{\mathbb{Z},c,s}(x) = \rho_{c,s}(x)/\rho_{c,s}(\mathbb{Z})$$

where $\rho_{c,s}(\mathbb{Z}) = \sum_{z\in\mathbb{Z}} \rho_{c,s}(z)$.

In the above definition, the denominator $\rho_{c,s}(\mathbb{Z})$ is for normalization. For convenience, we may omit c for $c = 0$, e.g. $\rho_{0,s}(x) = \rho_s(x)$ and $D_{\mathbb{Z},0,s}(x) = D_{\mathbb{Z},s}(x)$.

Gaussian sampling over integers $\mathbb{Z}$ can be formulated as a multilevel coding problem over a binary partition chain $\mathbb{Z}/2\mathbb{Z}/4\mathbb{Z}/\cdots 2^r\mathbb{Z}/\cdots$ of which each level is labeled by $X_1, X_2, \ldots, X_r, \ldots$ (see Fig. 3). Then the discrete Gaussian distribution over integers $D_{\mathbb{Z},c,s}$ induces a distribution $P_{X_{1:r}}$ whose limit corresponds to $D_{\mathbb{Z},c,s}$ as r goes to infinity. By cutting off the tail of negligible probability, a discrete Gaussian distribution over the integer lattice $\mathbb{Z}$ can be reduced to a distribution over a finite set. An example is $D_{\mathbb{Z},s=3\sqrt{2\pi}}$ for which a constellation of 32 points centred at 0 is somewhat sufficient because the total probability is rather close to 1.

[3]The SC decoding works effectively for both symmetric and asymmetric channels. In order to keep it consistent with the SC decoder in [21], we symmetrize (X, Y) to calculate $P_{U^{(i)}|Y^{1:N},U^{1:i-1}}$.

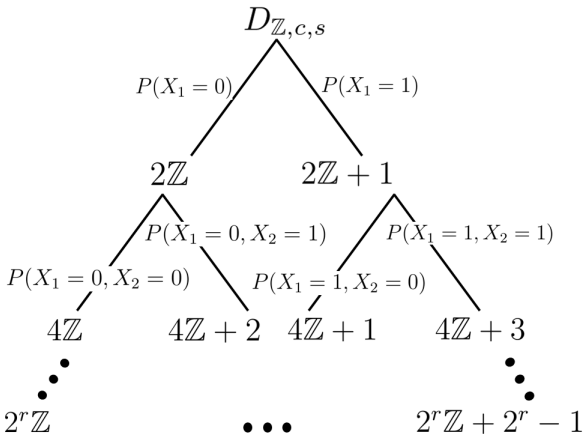

Fig. 3. An r-level binary partition tree of the integer lattice $\mathbb{Z}$.

Suppose r levels of partition are employed to approximate $D_{\mathbb{Z},c,s}$. The chain rule of conditional probability and the chain rule of conditional entropy, i.e.

$$P(X_{1:r}) = \prod_{k=1}^{r} P(X_k|X_{1:k-1}), \tag{19}$$

$$H(X_{1:r}) = \sum_{k=1}^{r} H(X_k|X_{1:k-1}), \tag{20}$$

imply that the Gaussian distribution over the finite constellation can be generated in a level-by-level way. For the k-th level, we can generate the component source X_k by the the scheme proposed in Subsection II-C given the samples $x_{1:k-1}$ from lower levels as side information. The sampling problem for each level can be divided into two stages, construction and implementation.

For the first level, we want to generate the component source X_1 in the absence of any side information.

1) *Construction:* By performing the source polarization transformation G_N on N i.i.d. copies of X_1, we obtain an N dimensional vector $U_1^{1:N} = X_1^{1:N}G_N$. For any $\beta \in (0, 1/2)$ and $\alpha = 2^{-N^\beta}$, we formally define two sets $\mathcal{H}_{X_1}$ and $\mathcal{L}_{X_1}$ as

$$\mathcal{H}_{X_1} = \left\{ i \in [N] : \ Z(U_1^{(i)} \mid U_1^{1:i-1}) \in (1-\alpha, 1] \right\} \tag{21}$$

and

$$\mathcal{L}_{X_1} = \left\{ i \in [N] : \ Z(U_1^{(i)} \mid U_1^{1:i-1}) \in [0, \alpha) \right\}. \tag{22}$$

For any $i \in \mathcal{H}_{X_1}$, $U_1^{(i)}$ is approximately uniform and independent of $U_1^{1:i-1}$, while for $i \in \mathcal{L}_{X_1}$, $U_1^{(i)}$ is almost deterministic given the knowledge of $U_1^{1:i-1}$.

2) *Implementation:* After getting the two sets $\mathcal{H}_{X_1}$ and $\mathcal{L}_{X_1}$, we can generate N i.i.d. copies of X_1 by applying the polarization transform circuit to the input vector $U_1^{1:N}$ of which each entry takes a value according to the following rule:

$$U_1^{(i)} = \begin{cases} \text{Bernoulli}(\frac{1}{2}) & \text{if } i \in \mathcal{H}_{X_1} \\ \arg\max_{u_1^{(i)}} P_{U_1^{(i)}|U_1^{1:i-1}}(u_1^{(i)}|u_1^{1:i-1}) & \text{if } i \in \mathcal{L}_{X_1} \end{cases}, \tag{23}$$

and

$$U_1^{(i)} = \begin{cases} 0 \ w.p. \ P_{U_1^{(i)}|U_1^{1:i-1}}(0|u_1^{1:i-1}) \\ 1 \ w.p. \ P_{U_1^{(i)}|U_1^{1:i-1}}(1|u_1^{1:i-1}) \end{cases} \quad \text{if } i \in \mathcal{H}_{X_1}^c \backslash \mathcal{L}_{X_1} \ . \tag{24}$$

As discussed in Subsection II-C, by converting the source X_1 without side information to a BMS source pair $(\tilde{X}_1, X_1 \oplus \tilde{X}_1)$, we can calculate the Bhattacharyya parameter $Z(U_1^{(i)} \mid U_1^{1:i-1})$ and the posterior probability $P_{U_1^{(i)}|U_1^{1:i-1}}$ efficiently. Once we have a realization $u_1^{1:N}$ of $U_1^{1:N}$, we can obtain a realization $x_1^{1:N} = u_1^{1:N} G_N$ of $X_1^{1:N}$ and transmit it to the next level for further processing.

For higher levels with $k \in (1, r]$, our task is to generate N i.i.d. copies of source X_k given the side information $x_{1:k-1}^{1:N}$ which were generated at the previous $k-1$ levels.

1) *Construction:* By performing the source polarization transformation G_N on N i.i.d. copies of X_k, we obtain an N dimensional vector $U_k^{1:N} = X_k^{1:N} G_N$. For $\beta \in (0, 1/2)$ and $\alpha = 2^{-N^\beta}$, we define $\mathcal{H}_{X_k|X_{1:k-1}}$ and $\mathcal{L}_{X_k|X_{1:k-1}}$ as

$$\mathcal{H}_{X_k|X_{1:k-1}} = \left\{ i \in [N] : \ Z(U_k^{(i)} \mid X_{1:k-1}^{1:N}, U_k^{1:i-1}) \in (1-\alpha, 1] \right\} \tag{25}$$

and

$$\mathcal{L}_{X_k|X_{1:k-1}} = \left\{ i \in [N] : \ Z(U_k^{(i)} \mid X_{1:k-1}^{1:N}, U_k^{1:i-1}) \in [0, \alpha) \right\}. \tag{26}$$

2) *Implementation:* We can generate N i.i.d. copies of X_k by applying the polarization transformation circuit to the input vector $U_k^{1:N}$ of which each entry takes a value according to the following rule:

$$U_k^{(i)} = \begin{cases} \text{Bernoulli}(\frac{1}{2}) & \text{if } i \in \mathcal{H}_{X_k|X_{1:k-1}} \\ \arg\max_u P_{U^{(i)}|X_{1:k-1}^{1:N}, U_k^{1:i-1}}(u|x_{1:k-1}^{1:N}, u_k^{1:i-1}) & \text{if } i \in \mathcal{L}_{X_k|X_{1:k-1}} \end{cases} \tag{27}$$

and

$$U_k^{(i)} = \begin{cases} 0 \ w.p. \ P_{U_k^{(i)}|X_{1:k-1}^{1:N}, U_k^{1:i-1}}(0|x_{1:k-1}^{1:N}, u_k^{1:i-1}) \\ 1 \ w.p. \ P_{U_k^{(i)}|X_{1:k-1}^{1:N}, U_k^{1:i-1}}(1|x_{1:k-1}^{1:N}, u_k^{1:i-1}) \end{cases} \\ \text{if } i \in \mathcal{H}_{X_k|X_{1:k-1}}^c \backslash \mathcal{L}_{X_k|X_{1:k-1}}. \tag{28}$$

Once we have a realization $u_k^{1:N}$ of $U_k^{1:N}$, we can obtain a realization $x_k^{1:N} = u_k^{1:N} G_N$ of $X_k^{1:N}$ and pass it to the next level for further processing. Again, $Z(U_k^{(i)} \mid X_{1:k-1}^{1:N}, U_k^{1:i-1})$ and $P_{U_k^{(i)}|X_{1:k-1}^{1:N}, U_k^{1:i-1}}$ can be calculated efficiently using Theorem 3. Note that for a target statistical difference between the ideal distribution and the one we can produce, the two sets $\mathcal{H}_{X_k|X_{1:k-1}}$ and $\mathcal{L}_{X_k|X_{1:k-1}}$ for each level can be determined offline. By repeating the operations in (27) and (28) from level 2 to level r, we can finally obtain N samples $x^{1:N}$ from $D_{\mathbb{Z},c,s}$, i.e.,

$$x^{1:N} = \sum_{k=1}^{r} 2^{k-1} x_k^{1:N}. \tag{29}$$

Fig. 4 shows how this Gaussian sampler works at each level in terms of construction and implementation. It also shows how to combine the output of each level. At the construction stage, W designates the probability transition from X_k to $X_{1:k}$. A sub-transition $W_N^{(i)}$ is obtained by combining then spliting N copies of i.i.d. source pair $(X_k, X_{1:k-1})$. At this stage the Bhattacharyya parameters of $W_N^{(i)}$ are calculated to define $\mathcal{H}_{X_k|X_{1:k-1}}$ and $\mathcal{L}_{X_k|X_{1:k-1}}$. At the implementation stage, realizations of $U^{1:N}$ are produced according to the implementation rules (27) and (28). In Appendix C, we give the key functions invoked at the construction and implementation stage. Given the two parameters N and β, the closeness between the ideal distribution and the one our sampler can produce will be analysed in the next section.

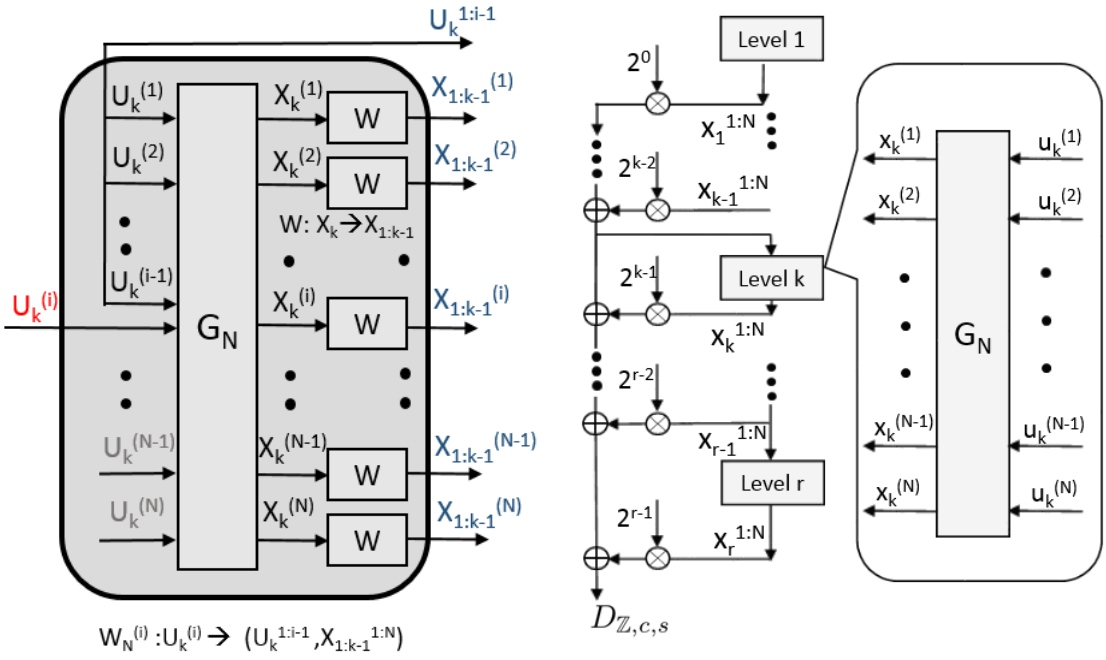

(a) (b)

Fig. 4. The construction and implementation of the polar sampler: (a) Construction (can run offline) (b) Implementation (runs online).

IV. Closeness Analysis

A. Closeness Measures

Definition 4 (Statistical distance): Denote by P and Q two distributions with countable supports and let $\mathcal{A}$ be the union of supports of P and Q. The SD between P and Q is

$$\mathbb{V}(P,Q)=\frac{1}{2}\sum_{a\in\mathcal{A}}|P(a)-Q(a)|.$$

Definition 5 (Kullback-Leibler divergence): Let P and Q be two distributions over a common countable set Ω, and let $\mathcal{A}\subset\Omega$ be the strict support of P ($P(a)>0$ iff $a\in\mathcal{A}$). The KL divergence D_{KL} of Q from P is defined as:

$$D_{KL}(P\|Q)=\sum_{a\in\mathcal{A}}P(a)\ln\left(\frac{P(a)}{Q(a)}\right)$$

with the convention that $\ln(x/0)=+\infty$ for any $x>0$.

B. The Approximation Error Model

In a concrete implementation, an ideal DGS is replaced by an approximation. To give a sharp estimation of the accuracy/security of a cryptographic primitive, the closeness between the approximation and the ideal DGS should be measured. Conventionally, the closeness between two distribution P and Q over the same support $\mathcal{A}$ is measured by the SD and KL divergence. In this section, we will derive the upper bounds on the closeness between the ideal DGS and the distribution generated by our sampling scheme in SD and KL divergence, respectively.

The approximation error comes from two sources, the tailcut (finite levels of the partition employed) and the polar source coding. On the one hand, we need to decide how many levels of partition are in need. On the other hand, the error introduced by polar sampling should also be analysed. Denote by $D_{\mathbb{Z},c,s}$ the target discrete Gaussian distribution and we decide to employ r levels of partition. If polar sampling did not introduce any error, we would generate a distribution $P_{X_{1:r}}$ with a closeness measure $\delta(D_{\mathbb{Z},c,s},P_{X_{1:r}})$ which is determined only by r for some metric δ. Then, let $Q_{X_{1:r}}(x_{1:r})$ denote the distribution obtained by polar sampling where the error introduced is $\delta(P_{X_{1:r}},Q_{X_{1:r}})$. By the triangle inequality of SD, we obtain the SD between the ideal discrete Gaussian distribution and ours as follows,

$$\mathbb{V}(D_{\mathbb{Z},c,s},Q_{X_{1:r}})\le\mathbb{V}(D_{\mathbb{Z},c,s},P_{X_{1:r}})+\mathbb{V}(P_{X_{1:r}},Q_{X_{1:r}}). \tag{30}$$

Since the KL divergence does not satisfy the triangle inequality, we will give $D(D_{\mathbb{Z},c,s}\|P_{X_{1:r}})$ and $D(P_{X_{1:r}}\|Q_{X_{1:r}})$ separately rather than a total KL divergence $D(D_{\mathbb{Z},c,s}\|Q_{X_{1:r}})$. However, as discussed in [7, Chapter 3] the lack of symmetry and triangle inequality can be easily handled in KL-based security analysis.

C. Approximation Error from Tailcut

Definition 6 (Smoothing Parameter [3]): For an n-dimensional lattice Λ, and positive real $\epsilon > 0$, we define its smoothing parameter $\eta_\epsilon(\Lambda)$ to be the smallest s such that $\rho_{1/s}(\Lambda^* \setminus \{0\}) \leq \epsilon$.

The smoothing parameter quantifies how large s is sufficient such that $D_{\Lambda,c,s}$ behaves like the continuous Gaussian distribution. It is implied by Definition 6 that for any $\epsilon > 0$, the smoothing parameter $\eta_\epsilon(\mathbb{Z})$ of $\mathbb{Z}$ is the smallest s such that $\rho(s\mathbb{Z}) \leq 1 + \epsilon$.

Lemma 1 (Lemma 4.2, [28]): For any $\epsilon > 0$, any $s > \eta_\epsilon(\mathbb{Z})$, and any $t > 0$,

$$\Pr_{x \leftarrow D_{\mathbb{Z},c,s}}(|\mathrm{x} - \mathrm{c}| \geq t \cdot s) \leq \frac{1+\epsilon}{1-\epsilon} \cdot 2e^{-\pi t^2}.$$

Instead of sampling over the full domain of the integer lattice, a distribution tail of negligible probability is cut off in practice. Suppose 2^r samples are left after the tailcut. Let $\mathcal{A} = \mathbb{Z} \cap [-2^{r-1} + c, 2^{r-1} + c)$. The distribution of the finite set is

$$\begin{aligned} D_\gamma(a) &= \frac{\rho_{c,s}(a)}{\sum_{a \in \mathcal{A}} \rho_{c,s}(a)} \\ &= D_{\mathbb{Z},c,s}(a) / D_{\mathbb{Z},c,s}(\mathcal{A}), \end{aligned}$$

where $a \in \mathcal{A}$ and γ is the probability of the tail. This constellation $\mathcal{A}$ of 2^r points can be represented as a binary partition tree labeled by $X_{1:r}$ in the same way as Fig. 3. In our sampling scheme, we obtain a sample labeled by

$$x^{1:N} = \sum_{k=1}^{r} 2^{k-1} x_k^{1:N}.$$

There exists a one-to-one mapping from $X_{1:r}$ to $\mathcal{A}$. Therefore $P_{X_{1:r}}$ and the tailcut distribution D_γ are exactly the same and we can obtain $\mathbb{V}(D_{\mathbb{Z},c,s}, P_{X_{1:r}})$ (resp. $D_{KL}(D_{\mathbb{Z},c,s} \| P_{X_{1:r}})$) by calculating $\mathbb{V}(D_{\mathbb{Z},c,s}, D_\gamma)$ (resp. $D_{KL}(D_{\mathbb{Z},c,s} \| D_\gamma)$).

1) SD-Based Analysis: Given the tailcut distribution D_γ over the finite constellation $\mathcal{A}$ as above, the SD between $D_{\mathbb{Z},c,s}$ and D_γ is

$$\begin{aligned} \mathbb{V}(D_{\mathbb{Z},c,s}, D_\gamma) &= \frac{1}{2} \sum_{a \notin \mathcal{A}} |D_{\mathbb{Z},c,s}(a) - 0| + \frac{1}{2} \sum_{a \in \mathcal{A}} |D_{\mathbb{Z},c,s}(a) - D_\gamma(a)| \\ &= \frac{1}{2}\gamma + \frac{1}{2} \sum_{a \in \mathcal{A}} \left| D_{\mathbb{Z},c,s}(a) \left(1 - \frac{1}{D_{\mathbb{Z},c,s}(\mathcal{A})}\right) \right| \\ &= \frac{1}{2}\gamma + \frac{1}{2}(1-\gamma) \left| 1 - \frac{1}{D_{\mathbb{Z},c,s}(\mathcal{A})} \right| \\ &= \frac{1}{2}\gamma + \frac{1}{2}(1-\gamma) \left| 1 - \frac{1}{1-\gamma} \right| \\ &= \gamma. \end{aligned}$$

By Lemma 1, the SD between $D_{\mathbb{Z},c,s}$ and $P_{X_{1:r}}$ is bounded as

$$\begin{aligned}\mathbb{V}(D_{\mathbb{Z},c,s}, P_{X_{1:r}}) &= \mathbb{V}(D_{\mathbb{Z},c,s}, D_\gamma) \\ &\leq \frac{1+\epsilon}{1-\epsilon} \cdot 2e^{-\pi t^2}, \end{aligned} \tag{31}$$

for any $\epsilon > 0$, $s > \eta_\epsilon(\mathbb{Z})$ and $t \cdot s = 2^{r-1}$.

2) KL-Based Analysis: Given the one-to-one mapping between $\mathcal{A}$ and $X_{1:r}$ and the tailcut setting as above, D_γ over the finite constellation $\mathcal{A}$ can be written in the form

$$\begin{aligned} P(X_{1:r} = x) &= D_{\mathbb{Z},c,s}(a) / \sum_{a \in \mathcal{A}} D_{\mathbb{Z},c,s}(a) \\ &= D_{\mathbb{Z},c,s}(a | a \in \mathcal{A}). \end{aligned}$$

The KL divergence between D_γ and $D_{\mathbb{Z},c,s}$ is

$$\begin{aligned} D_{KL}(D_\gamma \| D_{\mathbb{Z},c,s}) &= \sum_{a \in \mathcal{A}} D_{\mathbb{Z},c,s}(a|a \in \mathcal{A}) \ln \frac{D_{\mathbb{Z},c,s}(a|a \in \mathcal{A})}{D_{\mathbb{Z},c,s}(a)} \\ &= \sum_{a \in \mathcal{A}} D_{\mathbb{Z},c,s}(a|a \in \mathcal{A}) \ln \frac{D_{\mathbb{Z},c,s}(a|a \in \mathcal{A})}{D_{\mathbb{Z},c,s}(a|a \in \mathcal{A}) D_{\mathbb{Z},c,s}(x \in \mathcal{A})} \\ &= \sum_{a \in \mathcal{A}} D_{\mathbb{Z},c,s}(a|a \in \mathcal{A}) \ln \frac{1}{D_{\mathbb{Z},c,s}(a \in \mathcal{A})} \\ &= \ln \frac{1}{D_{\mathbb{Z},c,s}(a \in \mathcal{A})}. \end{aligned}$$

According to the second-order Taylor bound, if $D_{\mathbb{Z},c,s}(a \in \mathcal{A}) = 1-\gamma$ for any $0 < \gamma < 1$, $D_{KL}(D_\gamma \| D_{\mathbb{Z},c,s})$ is bounded by

$$\begin{aligned} D_{KL}(D_\gamma \| D_{\mathbb{Z},c,s}) &= \gamma + O(\gamma^2) \\ &\approx \mathbb{V}(P_{X_{1:r}}, D_{\mathbb{Z},c,s}). \end{aligned} \tag{32}$$

and so is $D_{KL}(P_{X_{1:r}} \| D_{\mathbb{Z},c,s})$.

D. Approximation Error from Polar Sampling

1) KL-Based Error Analysis: Let $P_{X_{1:r}^{1:N}}(x_{1:r}^{1:N})$ denote the distribution of N i.i.d. $X_{1:r}$ defined as above. For any $0 < \beta < 0.5$, $N = 2^n, n \geq 1$ and the corresponding high and low-entropy sets defined in (25) and (26), one can generate a distribution $Q_{X_{1:r}^{1:N}}(x_{1:r}^{1:N})$ using the rules (27) and (28). To give the KL divergence between $P_{X_{1:r}^{1:N}}(x_{1:r}^{1:N})$ and $Q_{X_{1:r}^{1:N}}(x_{1:r}^{1:N})$, we first modify the implementation rules (27) and (28) to

$$U_k^{(i)} = \begin{cases} 0 \ w.p. \ \frac{1}{2} \\ 1 \ w.p. \ \frac{1}{2} \end{cases} \quad \text{if } i \in \mathcal{H}_{X_k|X_{1:k-1}} \tag{33}$$

and

$$U_k^{(i)} = \begin{cases} 0 \ w.p. \ P_{U_k^{(i)}|X_{1:k-1}^{1:N},U_k^{1:i-1}}(0|x_{1:k-1}^{1:N}, u_k^{1:i-1}) \\ 1 \ w.p. \ P_{U_k^{(i)}|X_{1:k-1}^{1:N},U_k^{1:i-1}}(1|x_{1:k-1}^{1:N}, u_k^{1:i-1}) \end{cases} \quad \text{if } i \in \mathcal{H}^c{}_{X_k|X_{1:k-1}} \ , \tag{34}$$

where only the deterministic decisions for $U_k^{(i)}$ in $\mathcal{L}_{X_k|X_{1:k-1}}$ are replaced by random decisions. Let $Q'_{X_{1:r}^{1:N}}(x_{1:r}^{1:N})$ denote the distribution obtained from the implementation rules described in (33) and (34). The KL divergence between $P_{X_{1:r}^{1:N}}$ and $Q'_{X_{1:r}^{1:N}}$ is given as follows,

$$\begin{aligned} & D_{KL}(P_{X_{1:r}^{1:N}} \| Q'_{X_{1:r}^{1:N}}) \\ & \overset{(a)}{=} D_{KL}(P_{U_{1:r}^{1:N}} \| Q'_{U_{1:r}^{1:N}}) \\ & \overset{(b)}{=} D_{KL}(P_{U_1^{1:N}} P_{U_2^{1:N}|U_1^{1:N}} \cdots P_{U_r^{1:N}|U_{1:r-1}^{1:N}} \| Q'_{U_1^{1:N}} Q'_{U_2^{1:N}|U_1^{1:N}} \cdots Q'_{U_r^{1:N}|U_{1:r-1}^{1:N}}) \\ & \overset{(c)}{=} D_{KL}(P_{U_1^{1:N}} \| Q'_{U_1^{1:N}}) + D_{KL}(P_{U_2^{1:N}|U_1^{1:N}} \| Q'_{U_2^{1:N}|U_1^{1:N}}) + \cdots \\ & \qquad\qquad + D_{KL}(P_{U_r^{1:N}|U_{1:r-1}^{1:N}} \| Q'_{U_r^{1:N}|U_{1:r-1}^{1:N}}) \end{aligned} \tag{35}$$

where the equalities and inequalities are due to

(a) One-to-one mapping from $X_{1:r}^{1:N}$ to $U_{1:r}^{1:N}$;

(b) The chain rule of joint distribution;

(c) The chain rule of KL divergence.

For any level $k \in \{1, \cdots r\}$, $D_{KL}(P_{U_k^{1:N}|U_{1:k-1}^{1:N}} \| Q'_{U_k^{1:N}|U_{1:k-1}^{1:N}})$ is bounded as follows,

$$\begin{aligned} & D_{KL}(P_{U_k^{1:N}|U_{1:k-1}^{1:N}} \| Q'_{U_k^{1:N}|U_{1:k-1}^{1:N}}) \\ & \overset{(d)}{=} \sum_{i=1}^{N} D_{KL}(P_{U_k^{(i)}|U_k^{1:i-1},U_{1:k}^{1:N}} \| Q'_{U_k^{(i)}|U_k^{1:i-1},U_{1:k}^{1:N}}) \\ & \overset{(e)}{=} \sum_{i \in \mathcal{H}_k} D_{KL}(P_{U_k^{(i)}|U_k^{1:i-1},U_{1:k}^{1:N}} \| Q'_{U_k^{(i)}|U_k^{1:i-1},U_{1:k}^{1:N}}) \\ & \overset{(f)}{=} \sum_{i \in \mathcal{H}_k} \ln 2 \left[1 - H_P(U_k^{(i)}|U_k^{1:i-1}, U_{1:k}^{1:N})\right] \\ & \overset{(g)}{\leq} \sum_{i \in \mathcal{H}_k} \ln 2 \left[1 - Z_P(U_k^{(i)}|U_k^{1:i-1}, U_{1:k}^{1:N})^2\right] \\ & \overset{(h)}{\leq} 2 \ln 2 \cdot N 2^{-N^\beta}, \end{aligned} \tag{36}$$

where the equalities and inequalities are due to

(d) The chain rule of KL divergence;

(e) For $i \in \mathcal{H}^c_{X_k|X_{1:k-1}}$, $Q'(u_k^{(i)}|u_k^{1:i-1}, u_{1:k-1}^{1:N}) = P(u_k^{(i)}|u_k^{1:i-1}, u_{1:k-1}^{1:N})$;

(f) The definition of $D_{KL}(\cdot\|\cdot)$ and $Q'(U_k^{(i)}|u_k^{1:i-1}, u_{1:k-1}^{1:N}) = \frac{1}{2}$ for $i \in \mathcal{H}_{X_k|X_{1:k-1}}$;

(g) $Z(X|Y)^2 \leq H(X|Y)$ [22];

(h) (25).

According to (35) and (36), the KL divergence between $P_{X_{1:r}^{1:N}}$ and $Q'_{X_{1:r}^{1:N}}$ is bounded as

$$D_{KL}(P_{X_{1:r}^{1:N}} \| Q'_{X_{1:r}^{1:N}}) \leq 2 \ln 2 \cdot rN2^{-N^\beta}.$$

In a similar fashion, the KL divergence between $Q_{X_{1:r}^{1:N}}$ and $Q'_{X_{1:r}^{1:N}}$ is given as follows,

$$\begin{aligned}
&D_{KL}(Q_{X_{1:r}^{1:N}} \| Q'_{X_{1:r}^{1:N}}) \\
&= D_{KL}(Q_{U_{1:r}^{1:N}} \| Q'_{U_{1:r}^{1:N}}) \\
&= \sum_{k=1}^{r} \sum_{i=1}^{N} D_{KL}(Q_{U_k^{(i)}|U_k^{1:i-1},U_{1:k-1}^{1:N}} \| Q'_{U_k^{(i)}|U_k^{1:i-1},U_{1:k-1}^{1:N}}) \\
&\overset{(i)}{=} \sum_{k=1}^{r} \sum_{i \in \mathcal{L}_{X_k|X_{1:k-1}}} D_{KL}(Q_{U_k^{(i)}|U_k^{1:i-1},U_{1:k-1}^{1:N}} \| Q'_{U_k^{(i)}|U_k^{1:i-1},U_{1:k-1}^{1:N}}) \\
&\overset{(j)}{=} \sum_{k=1}^{r} \sum_{i \in \mathcal{L}_{X_k|X_{1:k-1}}} \ln 2 \sum_{u_k^{1:i-1},u_{1:k-1}^{1:N}} -Q'(u_k^{1:i-1}, u_{1:k-1}^{1:N}) \log Q'(\bar{u}_k^{(i)}|U_k^{1:i-1}, U_{1:k-1}^{1:N}) \\
&\overset{(k)}{\leq} \sum_{k=1}^{r} \sum_{i \in \mathcal{L}_{X_k|X_{1:k-1}}} \ln 2 \cdot H_P(U_k^{(i)}|U_k^{1:i-1}, U_{1:k-1}^{1:N}) \\
&\overset{(l)}{\leq} \sum_{k=1}^{r} \sum_{i \in \mathcal{L}_{X_k|X_{1:k-1}}} \ln 2 \cdot Z(U_k^{(i)}|U_k^{1:i-1}, U_{1:k-1}^{1:N}) \\
&\overset{(m)}{\leq} \ln 2 \cdot rN2^{-N^\beta}, \qquad (37)
\end{aligned}$$

where the equalities and inequalities come from

(i) For $i \in \mathcal{L}^c_{X_k|X_{1:k-1}}$, $Q'(u_k^{(i)}|u_k^{1:i-1}, u_{1:k-1}^{1:N}) = Q(u_k^{(i)}|u_k^{1:i-1}, u_{1:k-1}^{1:N})$;

(j) The definition of $D_{KL}(\cdot\|\cdot)$ (see Appendix B);

(k) See Appendix B;

(l) $H(X|Y) \leq Z(X|Y)$ [24];

(m) (26).

If m samples are picked randomly from all the N samples produced by our sampler, we can bound the KL divergence of the m-dimensional distributions by the additivity property as follows,

$$D_{KL}(P_{X_{1:r}^{1:m}} \| Q'_{X_{1:r}^{1:m}}) \leq \ln 2 \cdot r2N2^{-N^\beta} \text{and} \quad D_{KL}(Q_{X_{1:r}^{1:m}} \| Q'_{X_{1:r}^{1:m}}) \leq \ln 2 \cdot rN2^{-N^\beta},$$

for any $m \leq N$. Although we cannot give the KL divergence between $P_{X_{1:r}^{1:N}}$ and $Q_{X_{1:r}^{1:N}}$ due to the lack of triangle inequality, the absence of $D_{KL}(P_{X_{1:r}^{1:N}} \| Q_{X_{1:r}^{1:N}})$ will not prevent us from the security analysis which will be explained in the sequel.

2) SD-Based Error Analysis:

Theorem 4 (Polar Sampling Theorem): Let $P_{X_{1:r}^{1:N}}(x_{1:r}^{1:N})$ denote the distribution of N i.i.d. $X_{1:r}$ defined as above. For any $0 < \beta < 0.5$, $N = 2^n, n \geq 1$ and the corresponding high and low-entropy sets defined in (25) and (26), one can generate a distribution $Q_{X_{1:r}^{1:N}}(x_{1:r}^{1:N})$ using the rules (27) and (28), and the SD between $P_{X_{1:r}^{1:N}}(x_{1:r}^{1:N})$ and $Q_{X_{1:r}^{1:N}}(x_{1:r}^{1:N})$ is upper bounded as

$$\mathbb{V}(Q_{X_{1:r}^{1:N}}, P_{X_{1:r}^{1:N}}) \leq (\sqrt{2}+1)\sqrt{\frac{1}{2}\ln 2 \cdot rN2^{-N^\beta}}.$$

Proof 1: From the definition of Q' given in KL-based analysis, it is straightforward to obtain the SD between $\mathbb{V}(P_{X_{1:r}^{1:N}} \| Q'_{X_{1:r}^{1:N}}) \leq r2N2^{-N^\beta}$ by Pinsker's inequality as follows,

$$\begin{aligned}\mathbb{V}(P_{X_{1:r}^{1:N}} \| Q'_{X_{1:r}^{1:N}}) &\leq \sqrt{\frac{1}{2}\ D_{KL}(P_{X_{1:r}^{1:N}} \| Q'_{X_{1:r}^{1:N}})} \\ &\leq \sqrt{\ln 2 \cdot rN2^{-N^\beta}}.\end{aligned}$$

In a similar fashion, we obtain

$$\begin{aligned}\mathbb{V}(Q_{X_{1:r}^{1:N}} \| Q'_{X_{1:r}^{1:N}}) &\leq \sqrt{\frac{1}{2}\ D_{KL}(Q_{X_{1:r}^{1:N}} \| Q'_{X_{1:r}^{1:N}})} \\ &\leq \sqrt{\frac{1}{2}\ln 2 \cdot rN2^{-N^\beta}}.\end{aligned}$$

Since SD satisfies the triangle inequality and symmetry property, the SD between $P_{X_{1:r}^{1:N}}$ and $Q_{X_{1:r}^{1:N}}$ is bounded as

$$\mathbb{V}(Q_{X_{1:r}^{1:N}}, P_{X_{1:r}^{1:N}}) \leq (\sqrt{2}+1)\sqrt{\frac{1}{2}\ln 2 \cdot rN2^{-N^\beta}} \tag{38}$$

It can be observed from (30), (31), (38) that for sufficiently large N and properly chosen β and r, the distribution $Q_{X_{1:r}^{1:N}}$ generated by our sampler can well approximate $D_{\mathbb{Z}^{1:N},c,s}$. Usually, a cryptographic scheme needs many more than one sample at each run. For example, in the context of ring LWE-based encryption, each query to the oracle gives m discrete Gaussian samples where m is the dimension of the ring. If m samples are picked arbitrarily from all the N samples generated by our sampler, it can be verified that the SD of the two m-dimensional distributions is bounded by

$$\mathbb{V}(Q_{X_{1:r}^{1:m}}, P_{X_{1:r}^{1:m}}) \leq (\sqrt{2}+1)\sqrt{\frac{1}{2}\ln 2 \cdot rN2^{-N^\beta}}.$$

Remark 1: We claim the polar sampler to achieve the information theoretic optimality in a sense that as the block length N goes to infinity, the overall faction of high-entropy sets for each level approaches the entropy $H(D_{\mathbb{Z},c,s})$. Meanwhile, the randomness consumed to approximate the ideal $D_{\mathbb{Z},c,s}$ approaches $H(D_{\mathbb{Z},c,s})$ arbitrarily.

V. Security Analysis and Parameter Selection

Definition 7 (Standard cryptographic scheme [18]): We consider an arbitrary cryptographic scheme S, consisting of one or more algorithms with oracle access to a probability distribution ensemble $\mathcal{P}_\theta$, and whose security against an adversary A (also consisting of one or more algorithms) is described in terms of a game $G^{\mathcal{P}}_{S,A}$ defining the event that A succeed in breaking the scheme S. The success probability of A against S (when using samples from $\mathcal{P}_\theta$) is defined as $\epsilon^{\mathcal{P}}_A = \Pr\{G^{\mathcal{P}}_{S,A}\}$. The cost of an attack A against S is defined as $t_A/\epsilon^{\mathcal{P}}_A$, and the bit-security of S is the minimum (over all adversaries A) of $\log(t_A/\epsilon^{\mathcal{P}}_A)$.

Lemma 2 ([18]): Let $S^{\mathcal{P}}$ be a standard cryptographic scheme as in Definition 7 with a black-box access to a probability distribution ensemble $\mathcal{P}_\theta$, and δ any cryptographically useful measure. If $S^{\mathcal{P}}$ is λ-bit secure and $\delta(\mathcal{P}_\theta, \mathcal{Q}_\theta) \leq 2^{-\lambda}$, then $S^{\mathcal{Q}}$ is $(\lambda-1)$-bit secure.

Lemma 2 illustrates how the security level of a standard cryptographic scheme with respect to an ideal distribution is related to that with respect to an approximated distribution. To approximate a λ-bit secure scheme $S^{\mathcal{P}}$ with a $(\lambda-1)$-bit secure scheme $S^{\mathcal{Q}}$, one needs to guarantee that $\delta(\mathcal{P}_\theta, \mathcal{Q}_\theta) \leq 2^{-\lambda}$ for some useful metrics e.g. SD, KL, etc. Following the settings of $\mathcal{D}_{\mathbb{Z}^m,c,s}$ and $\mathcal{Q}_{X^{1:m}_{1:r}}$ as in Section IV, for a $(\lambda+1)$-bit secure standard cryptographic scheme $S^{\mathcal{D}_{\mathbb{Z}^m,c,s}}$, we can replace $\mathcal{D}_{\mathbb{Z}^m,c,s}$ by $\mathcal{Q}_{X^{1:m}_{1:r}}$ incurring only 1 bit of security loss if it is satisfied that $\delta(\mathcal{D}_{\mathbb{Z},c,s}, \mathcal{Q}_{X^{1:m}_{1:r}}) \leq 2^{-(\lambda+1)}$. Moreover, the useful metrics should satisfy the properties of probability preservation, sub-additivity and data processing inequality [18].

A. Security Analysis with SD

As analysed in Section IV, the SD between the ideal DGS and the one we generate vanishes exponentially with block-length N for any $\beta \in (0, 0.5)$ and an appropriate choice of r. If we apply our DGS algorithm to a standard cryptographic scheme as in Definition 7, we are supposed to choose N, β and r properly to achieve the desired closeness subject to the security requirement and the limitation on resources. And we regard Lemma 2 as the guideline by which we can evaluate the target closeness based on a target security level.

Suppose we expect a λ-bit secure scheme $\mathcal{S}^{\mathcal{Q}_{X^{1:m}_{1:r}}}$ as a substitution of $S^{\mathcal{D}_{\mathbb{Z}^m,c,s}}$. According to equation (30), the overall SD between $D_{\mathbb{Z}^m,c,s}$ and $Q_{X^{1:m}_{1:r}}$ breaks down into $\mathbb{V}(D_{\mathbb{Z}^m,c,s}, P_{X^{1:m}_{1:r}})$ caused by tailcut and $\mathbb{V}(P_{X^{1:m}_{1:r}}, Q_{X^{1:m}_{1:r}})$ caused by polar coding. Lemma 2 suggests that $\mathbb{V}(D_{\mathbb{Z}^m,c,s}, Q_{X^{1:m}_{1:r}})$ should be no larger than $2^{-(\lambda+1)}$, therefore both $\mathbb{V}(D_{\mathbb{Z}^m,c,s}, P_{X^{1:m}_{1:r}})$ and $\mathbb{V}(P_{X^{1:m}_{1:r}}, Q_{X^{1:m}_{1:r}})$ should be no larger than $2^{-(\lambda+2)}$. The sub-additivity of SD helps establish the bound of $\mathbb{V}(D_{\mathbb{Z}^m,c,s}, P_{X^{1:m}_{1:r}})$ for Lemma 1. More specifically, a tailcut of $D_{\mathbb{Z}^m,c,s}$ with support $\mathbb{Z} \cap [c - ts,\ c + ts]$ for each independent dimension of $\mathbb{Z}^m$ is a good approximation of $D_{\mathbb{Z}^m,c,s}$ with $\mathbb{V}(D_{\mathbb{Z}^m,c,s}, P_{X^{1:m}_{1:r}}) \leq 2^{-(\lambda+2)}$ if we set $t \approx \sqrt{(\lambda + \log m + 2)\ln 2/\pi}$ for

$s > \eta_\epsilon(\mathbb{Z})$; accordingly the number of levels r should be no less than $\left\lceil \log(2s\sqrt{(\lambda + \log m + 2)\ln 2/\pi}) \right\rceil$. By Theorem 4, the SD between $P^{1:m}_{X_{1:r}}$ and $Q^{1:m}_{X_{1:r}}$ is bounded with only a small loss in tightness by

$$\mathbb{V}(P_{X^{1:m}_{1:r}}, Q_{X^{1:m}_{1:r}}) \leq 2^{-2^{n\beta-1}+\frac{1}{2}n+\frac{1}{2}\log r+1}.$$

for $m \leq N$ and $N = 2^n$. Therefore, we can guarantee that $\mathbb{V}(P_{X^{1:m}_{1:r}}, Q_{X^{1:m}_{1:r}}) \leq 2^{-(\lambda+2)}$ by making $2^{-2^{n\beta-1}+\frac{1}{2}n+\frac{1}{2}\log r+1} \leq 2^{-(\lambda+2)}$ for $\beta \in (0, 0.5)$. The number of levels r is determined once s and t is fixed, while n and β should be chosen properly to minimize the cost of memory and running time subject to the security requirement.

As mentioned earlier, our algorithm consists of two stages: construction and implementation. The former is done offline and the latter runs online. At the implementation stage, the running time to produce one bit $U^{(i)}_k$ varies with respect to different sets due to different implementation rules by which $U^{(i)}_k$ is generated either randomly or deterministically. The parameter β affects the running time to produce $U^{1:N}_k$ as it defines the high and low entropy sets. n is obviously in a more dominant position because it greatly influences the two stages with respect to the efficiency of both computational and memory cost. Given multiple parameter options to achieve a target security level, we suggest to give high priority to the one with the smallest n (or N) for the sake of efficiency. Fig. 5 illustrates how security level λ of a scheme is related to β and n given that the scheme with access to a perfect distribution $D_{\mathbb{Z}^m,c,s}$ is $(\lambda+1)$-bit secure. A large n means a deep polarization effect giving rise to small closeness loss for the two polarized sets. Meanwhile, a large β will define two relatively small polarized sets which is also good to the closeness. There is no surprise that the two graphs only have minor differences because a relatively small r suffices to meet the requirement of $\mathbb{V}(D_{\mathbb{Z}^{1:m},c,s}, P_{X^{1:m}_{1:r}}) \leq 2^{-(\lambda+2)}$ for a large s.

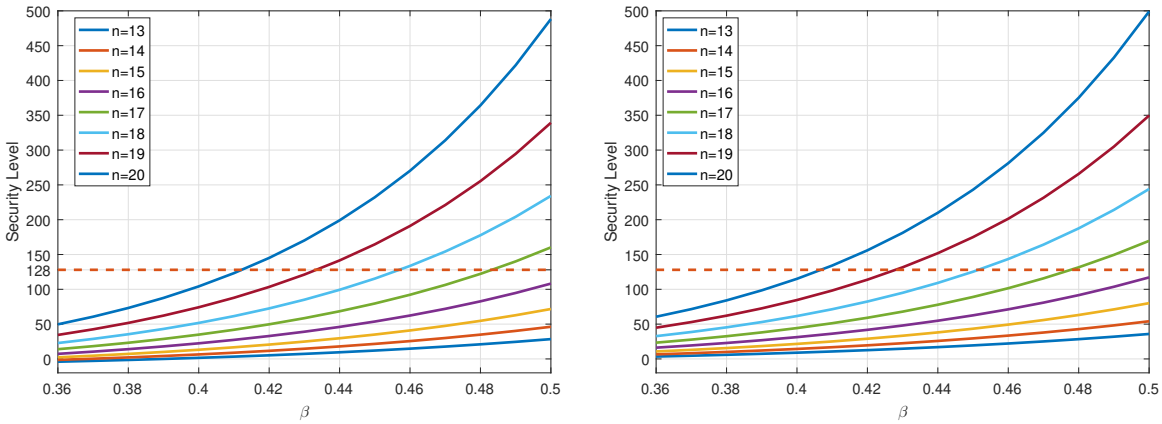

Fig. 5. The relation between security level of a scheme and β, n based on SD analysis: (a) s=8. (b) s=2^{10}.

B. Security Analysis with KL Divergence

Lemma 3 (Bounding Success Probability Variations, [6]): Let $\mathcal{E}^{\mathcal{P}}$ be an algorithm making at most q queries to an oracle sampling from a distribution $\mathcal{P}$ and returning a bit. Let $\epsilon \geq 0$, and $\mathcal{Q}$ be a distribution such that $D_{KL}(\mathcal{P}\|\mathcal{Q}) < \epsilon$. Let x (resp. y) denote the probability that $\mathcal{E}^{\mathcal{P}}$ (resp. $\mathcal{E}^{\mathcal{Q}}$) outputs 1. Then, $|x-y| \leq \sqrt{q\epsilon/2}$.

Security argument [7]: It can be concluded from Lemma 3 that if a scheme is λ-bit secure with oracle access to a perfect distribution $\mathcal{P}$ and the KL divergence between $\mathcal{P}$ and another distribution $\mathcal{Q}$ satisfies $D_{KL}(\mathcal{P}\|\mathcal{Q}) \leq 2^{-\lambda}$, then this scheme is also about λ-bit secure with oracle access to $\mathcal{Q}$. Note that this security argument holds only if $\mathcal{E}$ is a search problem but not a decisional one. The security argument based on KL divergence satisfies symmetry and triangle inequality though KL divergence itself does not (see Section 3.2 in [7] for detail).

Consider that a scheme with access to a perfect distribution $D_{\mathbb{Z}^m,c,s}$ is λ-bit secure. An adversary calls the sampler m times at each query for $m \leq$ the block-length N of polar codes in our sampling algorithm. Applying the additivity of KL divergence to (32), we have $D_{KL}(D_{\mathbb{Z}^{1:m},c,s}\|P_{X_{1:r}^{1:m}}) \leq m(\varepsilon+\varepsilon^2)$. In order to achieve λ-bit security after the tailcut, we need to set $m(\varepsilon+\varepsilon^2) \approx 2^{-\lambda}$ by selecting $t \approx \sqrt{(\lambda+\log m)\ln 2/\pi}$. The number of levels needed is therefore $r = \lceil \log(2t \cdot s) \rceil$. It is observed that KL divergence is almost the same as SD when used to analyse the tailcut error and the number of partition levels r. As given in Section IV-D1, the approximation error introduced by polar coding is determined by both $D_{KL}(P_{X_{1:r}^{1:m}}\|Q'_{X_{1:r}^{1:m}})$ and $D_{KL}(Q'_{X_{1:r}^{1:m}}\|P_{X_{1:r}^{1:m}})$ which are upper bounded as

$$D_{KL}(P_{X_{1:r}^{1:m}}\|Q'_{X_{1:r}^{1:m}}) \leq 2\ln 2 \cdot rN2^{-N^{\beta}}, \quad D_{KL}(Q_{X_{1:r}^{1:m}}\|Q'_{X_{1:r}^{1:m}}) \leq \ln 2 \cdot rN2^{-N^{\beta}}.$$

In order to preserve λ-bit security after $P_{X_{1:r}^{1:m}}$ is replaced by $Q_{X_{1:r}^{1:m}}$, we need to select $n = \log N$ and β properly such that $2^{-2^{n\beta}+n+\log(r)+1} \approx 2^{-\lambda}$. Fig. 6 shows how the security level is related to n, β in terms of different s. KL divergence shows its advantage over SD when used to analyse the approximation error from polar coding. To achieve the same security level, we can choose much smaller β and n than those obtained according to SD-based analysis, which will lead to a great reduction in both memory and running time.

Remark 2: As mentioned in Subsection II-C, we employ the upgrading and degrading merge algorithm to efficiently calculate the Bhattacharyya parameters with tolerable loss of accuracy [25]. How this inaccuracy affects the security level is given in Appendix D.

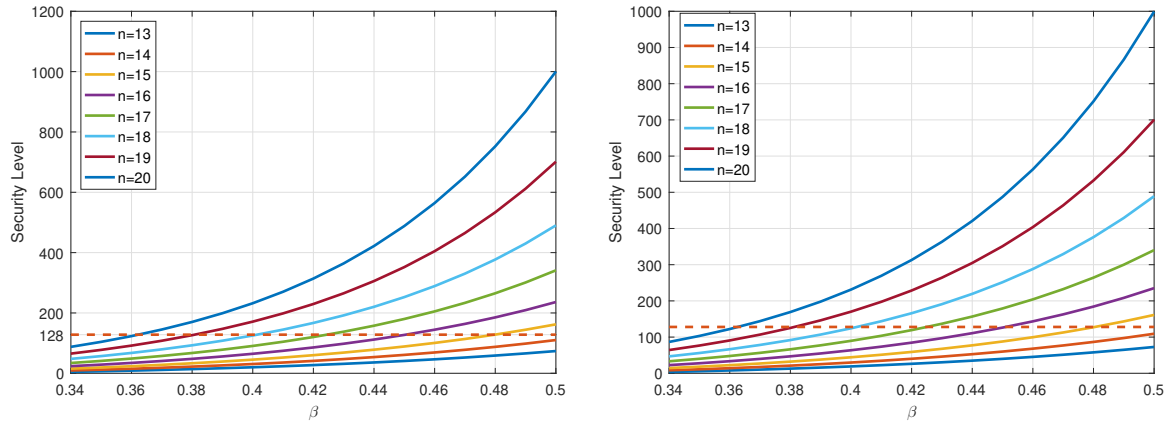

(a) (b)

Fig. 6. The relation between security level of a scheme and β, n based on KL analysis: (a) s=8. (b) s=2^{10}.

C. Security Analysis of Tailcut With Rényi Divergence

Definition 8 (Rényi divergence): Let P, Q be two distributions with supports $\mathcal{S}_P$ and $\mathcal{S}_Q$, respectively. Let $\mathcal{S}_P \subseteq \mathcal{S}_Q$. For $a \in (1, +\infty)$, we define the Rényi divergence of order a by

$$R_a(P\|Q) = \left(\sum_{x \in \mathcal{S}_P} \frac{P(x)^a}{Q(x)^{a-1}} \right)^{\frac{1}{a-1}}.$$

In [8], a sharper bound on security based on Rényi divergence is given under the assumption that the number of adversary queries q to an λ-bit secure scheme is far less than 2^λ. In NIST's proposals for post-quantum cryptography, it is assumed that $q \leq 2^{64}$ and any attacker making more than 2^{64} queries is impractical because it is easily detectable. Denote by $\mathcal{Q}$ and $\mathcal{Q}_\gamma$ a distribution and its tailcut such that $\frac{\mathcal{Q}_\gamma}{\mathcal{Q}} \leq 1+\gamma$ over the support $\mathcal{T}$ of $\mathcal{Q}_\gamma$ for some $\gamma \geq 1 - \mathcal{Q}(\mathcal{T})$. It is proved in [8] that $R_a(\mathcal{Q}_\gamma\|\mathcal{Q}) \leq 1+\gamma$. Consider a cryptographic scheme with λ bits of security and the number of queries to $\mathcal{Q}$ verifies $q \leq 2^{64}$. By the security argument in [8], this scheme is believed to lose at most one bit of security if $\mathcal{Q}$ is replaced by $\mathcal{Q}_\gamma$ provided that

$$R_a(\mathcal{Q}_\gamma\|\mathcal{Q}) \leq 1 + \frac{1}{4q} \text{ for } a = 2\lambda.$$

In implementation, we only need to guarantee that

$$\frac{\mathcal{Q}_\gamma}{Q} \leq 1 + \gamma \text{ for } \gamma = \frac{1}{4q}.$$

In the context of polar sampling, a $(\lambda+1)$-bit secure scheme $S^{\mathcal{D}_{\mathbb{Z}^m,c,s}}$ will be at least λ-bit secure when the ideal distribution $D_{\mathbb{Z},c,s}$ is replaced by its tailcut $P_{X_{1:r}}$ for $\lambda = 128$, $q = 2^{64}$ and $a = 2\lambda$ by taking

$$t \approx \sqrt{\frac{\ln 2(66 + \log m)}{\pi}}$$

and the number of levels needed is

$$r = \left\lceil \log \left(2s \sqrt{\frac{(66 + \log m) \ln 2}{\pi}} \right) \right\rceil .$$

Compared with the SD and KL-based analysis of tailcut, Rényi divergence contributes to a reduction on r by at most 1 level.

VI. Complexity and Comparison

A. A Constant-Time Algorithm

Efforts have been made to develop constant-time solutions to existing samplers e.g. [29], [15] as well as proposing new ones endowed with this desired quality against timing analysis attacks. At the implementation stage of polar sampling, the overall consumption of running time is dominated by two types of operations: calculating the LRs by SC decoding level by level and producing binary samples $U_{1:r}^{1:N}$ following the implementation rules as in (27) and (28). As distinguished from previous samplers, the polar sampler relies on a recursive transform on N inputs and yields N samples at each run. For a fixed block-length N, no matter what the distribution is, the SC decoding at each level requires exactly $N(1 + \log N)$ steps of LR calculations where two LRs are assembled to give a new one (Appendices A and C). Drawing binary samples according to (27) and (28) can also be made constant-time. On the one hand, drawing a bit in constant time uniformly at random or deterministically according to (27) is easy and cheap. On the other hand, sampling from a distribution statistically $2^{-\lambda}$-close to a Bernoulli variable $\mathcal{B}_p$ in (28) for a given bias p is also easy: take an approximation of p up to λ correct bits, then sample a uniform real $q \in [0, 1)$ up to λ bits of precision and answer 1 if and only if $q < p$ [10]. Moreover the fraction of unpolarized indexes vanishes as N tends to ∞. In conclusion, the implementation stage shown in Fig. 4 is block-wise constant in time if the two conditions below are satisfied:

- The number of levels r and the number of DGS samples N for the algorithm to produce at each run are fixed. Seeing that r is only related to the width s of $D_{\mathbb{Z},c,s}$ and the security level λ but has nothing to do with c, we claim the polar sampler to be constant-time for fixed s no matter what c is.
- The parameter β for each level is chosen properly such that $\mathcal{H}$, $\mathcal{L}$ and $\mathcal{H}^c \backslash \mathcal{L}$ for each level are fixed.

B. Time Complexity

The latest trend of DGS solutions is to expand a base sampler into one for arbitrary parameters. For example, the Knuth-Yao and CDT sampler can work as a base sampler to produce samples which are then combined into new samples with a relatively large standard deviation in a convolutional manner

[18], [30]. The polar sampler also admits such an extension for potential speedup and the focus of this subsection is to compare the polar sampler with other base samplers. Karmakar et al. [15] compared the time complexity of Knuth-Yao and CDT showing that the former can be made more time-saving. Therefore, it is fair to compare the polar sampler only with Knuth-Yao and we used a non constant-time Knuth-Yao implemented in C++[4] as well as its constant-time version[5]. We also perform benchmarks of a prototype polar sampler in terms of different choices of parameter s in C++.

The experiment is conducted on a PC with Ubtuntu 18.04 and an intel i9-9900K processor running at 3.60 GHz using one core. We use g++ to compile both Knuth-Yao and our implementation with compilation flag -Ofast enabled. For the benchmarks, we select $s \in \sqrt{2\pi} \cdot \{3, 8, 32, 256\}$ and the target security level $\lambda = 64$. According to the KL-based security analysis, we specify β to achieve 64 bits of security with respect to $N \in \{2^{13}, 2^{14}, 2^{15}\}$, and we select $r = \lceil \log(2st) \rceil$ where $t \approx \sqrt{(\lambda + \log m) \ln 2/\pi}$. We assume that one query to the sampling algorithm can obtain $m = 1024$ integer samples. The simulation results are shown in Table I. Firstly, the polar sampler always outperforms Knuth-Yao in speed with respect to the above setting. Secondly, Knuth-Yao slows down almost linearly as 2^r grows while the polar sampler still provides a competitive speed. This advantage stems from the binary partition of the integers. Thirdly, the polar sampler shows modest speed reduction as the block-length increases from 2^{14} to 2^{15}. This doesn't contradict the asymptotic information optimality claim which implies less randomness consumption per sample for larger N. The polarization effect can reduce the consumption of randomness to the optimum and contributes to the speed. However, the overall running time, in the current implementation, is dominated by the block-length. If N is not large enough such that the N source pairs are not polarized deeply enough, the acceleration gained from polarization may not be able to compensate for the slowdown induced by the increase of N.

In addition to the simulation results, we also compare the polar sampler with Micciancio and Walter's sampler [18] regarding the computational complexity. To yield one discrete Gaussian sample, a polar sampler carries out, on average, $O(\log s) \cdot (1 + \log N)$ arithmetic operations to update the LRs plus drawing $O(\log s)$ binary samples following (27) and (28). In the context of Micciancio and Walter's sampler SAMPLEZ, it performs two main subroutines sequentially, i.e. SAMPLEI and SAMPLEC. SAMPLEI combines small samples into a distribution of a larger standard deviation s and it consumes $O(\log s)$ invocations of a base sampler SAMPLEB which draws small samples from $\mathcal{D}_{c_0+\mathbb{Z},s_0}$ for $c_0 \in \mathbb{Z}/b$ and a relatively small s_0, e.g. Knuth-Yao. SAMPLEC is used to adjust the distribution center into a target c

[4]https://github.com/AaronHall4/BKW-Algorithm

[5]https://github.com/jnortiz/HIBE-Gaussian-Sampling

TABLE I

COMPARISON OF TIME EFFICIENCY BETWEEN THE POLAR SAMPLER AND KNUTH-YAO.

2^r	s	Knuth-Yao (samples/second)		polar sampler (samples/second)		
		constant-time	non constant-time	$N = 2^{13}$	$N = 2^{14}$	$N = 2^{15}$
2^6	$3\sqrt{2\pi}$	2.809E5/s	3.876E5/s	$\beta = 0.487$ 1.333E6/s	$\beta = 0.4535$ 1.283E6/s	$\beta = 0.4244$ 1.168E6/s
2^7	$8\sqrt{2\pi}$	1.172E5/s	2.212E5/s	$\beta = 0.4876$ 1.194E6/s	$\beta = 0.454$ 1.097E6/s	$\beta = 0.425$ 1.010E6/s
2^9	$32\sqrt{2\pi}$	3.255E4/s	6.017E4/s	$\beta = 0.488$ 0.960E6/s	$\beta = 0.4544$ 0.861E6/s	$\beta = 0.4252$ 0.792E6/s
2^{12}	$256\sqrt{2\pi}$	4.464E3/s	6.760E3/s	$\beta = 0.4885$ 0.680E6/s	$\beta = 0.455$ 0.621E6/s	$\beta = 0.4257$ 0.572E6/s

and it consumes k invocations of SAMPLEB where k represents the precision of $c \in b^{-k}\mathbb{Z}$. On average, SAMPLEZ consumes $O(\log s)+k$ invocations of SAMPLEB per discrete Gaussian sample. In an asymptotic sense, when N is sufficiently large the polar sampler spends barely on binary sampling but calculating the LRs which is believed to be easy compared with SAMPLEB. From a practical point of view, the simulation results also imply that for appropriate block-length N calculating the LRs plus sampling from (27) and (28) is more time-saving than a Knuth-Yao SAMPLEB on average, and so is the overall consumption.

C. Memory Cost

At the construction stage, one calculates the Bhatacharyya parameters using the upgrading and degrading merge techniques in [25] to find the indexes of the high, low-entropy and unpolarized sets. We employ a 2-bit flag to specify which set an index i is in. Given the number of levels r and block-length N, to store all the flags requires $\frac{rN}{4}$ bytes in total.

We also need to store a likelihood ratio table of the symmetrized channel, e.g. $LR(x_{1:k-1}, x_k) = \frac{W(x_k=0|x_{1:k-1})}{W(x_k=1|x_{1:k-1})}$ for $k \leq r$. The table consists of 2^r data for all the r levels. The likelihood ratio is stored in natural order of $X_{1:k-1}$ such that once the samples for the first $k-1$ levels $X_{1:k-1}^{1:N}$ are ready we can find the corresponding likelihood ratio by the index $x_{1:k}$ without scanning the table.

In addition, as shown in Appendix C, the polar sampler will create a floating point array of size $N \times (n+1)$ and a bit array of the same size to store instant data. Fortunately, the space-efficient SC decoding proposed in [31] greatly reduces the array size to $N \times 1$.

VII. Conclusions and Future Work

Our polar sampler is efficient, application-independent and constant-time. Our algorithm is effective in the case that when a large number of discrete Gaussian samples are required. The reduction in resources of random bits stems from the polarization process in which the randomness moves to the high-entropy set. For fixed parameters, the construction stage is prepared offline and the implementation stage is carried out online and constant in time. KL divergence is a more efficient metric than SD when used for security analysis of polar sampling. The Rényi divergence-based analysis of polar coding is still an open problem by now. It deserves more efforts to give a complete Rényi divergence-based analysis of our sampler and exploit the potential efficiency of Rényi divergence.

In this paper, we only use the basic 2×2 kernel, whose finite-length performance is not the best. Optimizing finite-length performance using other kernels of polar codes as well as various other issues are left to future work.

Appendix A
Computational Complexity of SC Decoding

Consider the SC decoding for an arbitrary polar code of length N. To estimate $u^{1:N}$ according to the rules given in (8), one needs to calculate the full set of LRs. Let $W : X \to Y$ denote a stochastic transition from the source X to side information Y with transition probability $W(Y|X) = P(Y|X)$. As shown in Fig. 1, the source polarization transform combines N i.i.d. copies of W in a recursive manner such that for any $0 \leq m \leq n$, $M = 2^m$, $N = 2^n$, $1 \leq \kappa \leq M/2$, the decoder calculates the LRs at the m-th layer of recursion as [21, Section VIII]

$$L_M^{(2\kappa-1)}(y_1^M, \hat{u}_1^{2\kappa-2}) = \frac{L_{M/2}^{(\kappa)}\left(y_1^{M/2}, \hat{u}_{1,o}^{2\kappa-2} \oplus \hat{u}_{1,e}^{2\kappa-2}\right) L_{M/2}^{(\kappa)}\left(y_{M/2+1}^{M}, \hat{u}_{1,e}^{2\kappa-2}\right) + 1}{L_{M/2}^{(\kappa)}\left(y_1^{M/2}, \hat{u}_{1,o}^{2\kappa-2} \oplus \hat{u}_{1,e}^{2\kappa-2}\right) + L_{M/2}^{(\kappa)}\left(y_{M/2+1}^{M}, \hat{u}_{1,e}^{2\kappa-2}\right)}, \tag{39}$$

and

$$L_M^{(2\kappa)}(y_1^M, \hat{u}_1^{2\kappa-1}) \left[L_{M/2}^{(\kappa)}\left(y_1^{M/2}, \hat{u}_{1,o}^{2\kappa-2} \oplus \hat{u}_{1,e}^{2\kappa-2}\right)\right]^{1-2\hat{u}_{2\kappa-1}} \cdot L_{M/2}^{(\kappa)}\left(y_{M/2+1}^{M}, \hat{u}_{1,e}^{2\kappa-2}\right). \tag{40}$$

where the notation $\hat{u}_{1,o}^{2\kappa-2}$ (resp. $\hat{u}_{1,e}^{2\kappa-2}$) represents a subvector of $\{\hat{u}^{(1)}, \cdots, \hat{u}^{(2\kappa-2)}\}$ with odd (resp. even) indexes. The stopping condition of the recursion is $L_1^{(1)}(y) = \frac{W(y|0)}{W(y|1)}$.

Observe that to calculate any LR pair $\left(L_M^{(2\kappa-1)}(y_1^M, \hat{u}_1^{2\kappa-2}), L_M^{(2\kappa)}(y_1^M, \hat{u}_1^{2\kappa-1})\right)$ at the m-th layer of the recursion, the decoder needs to know another LR pair $\left(L_{M/2}^{(\kappa)}(y_1^{M/2}, \hat{u}_{1,o}^{2\kappa-2} \oplus \hat{u}_{1,e}^{2\kappa-2}), L_{M/2}^{(\kappa)}(y_{M/2+1}^{M}, \hat{u}_{1,e}^{2\kappa-2})\right)$ at the (m-1)-th layer. The calculation of N LRs at layer m requires exactly N LR assembling at layer $m-1$. One can reversely compute the LRs layer by layer until he reaches the 0-th layer which is exactly the raw stochastic transition W. Suppose that assembling an LR pair of the $(m-1)$-th layer into one

LR of the m-th layer takes one complexity unit, then computing all the N LRs of the n-th layer requires $N(1+\log N)$ units. Fig. 7 gives an example of $N=8$.

APPENDIX B
KL DIVERGENCE FOR THE LOW-ENTROPY SET

For $i \in \mathcal{L}_{X_k|X_{1:k-1}}$, Q' and Q follow the distribution respectively as

$$Q'(u_k^{(i)}|u_k^{1:i-1}, u_{1:k-1}^{1:N}) = P(u_k^{(i)}|u_k^{1:i-1}, u_{1:k-1}^{1:N})$$

and

$$\begin{aligned}&Q(\bar{u}_k^{(i)}|u_k^{1:i-1}, u_{1:k-1}^{1:N}) = 1\\ &\text{for } \ \bar{u}_k^{(i)} = \arg\max_{u\in\{0,1\}} P_{U_k^{(i)}|X_{1:k-1}^{1:N}, U_k^{1:i-1}}(u|x_{1:k-1}^{1:N}, u_k^{1:i-1}).\end{aligned}$$

By definition of KL divergence, we have

$$\begin{aligned}&D_{KL}(Q_{U_k^{(i)}|U_k^{1:i-1}, U_{1:k-1}^{1:N}} \| Q'_{U_k^{(i)}|U_k^{1:i-1}, U_{1:k-1}^{1:N}})\\ &= \sum_{u_k^{1:i-1}, u_{1:k-1}^{1:N}} Q'(u_k^{1:i-1}, u_{1:k-1}^{1:N})[-1\cdot \log Q'(\bar{u}_k^{(i)}|u_k^{1:i-1}, u_{1:k-1}^{1:N})\\ &- 0\cdot\log(1-Q'(\bar{u}_k^{(i)}|u_k^{1:i-1}, u_{1:k-1}^{1:N})) + (0\log 0 + 1\log 1)].\end{aligned}$$

By definition Shannon entropy,

$$\begin{aligned}&H_P(U_k^{(i)}|U_k^{1:i-1}, U_{1:k-1}^{1:N})\\ &= -\sum_{u_k^{1:i-1}, u_{1:k-1}^{1:N}} Q'(u_k^{1:i-1}, u_{1:k-1}^{1:N}) \sum_{u_k^{(i)}} Q'(u_k^{(i)}|u_k^{1:i-1}, u_{1:k-1}^{1:N}) \log Q'(u_k^{(i)}|u_k^{1:i-1}, u_{1:k-1}^{1:N})\end{aligned}$$

for $i \in \mathcal{L}_{X_k|X_{1:k-1}}$. For $0.5 \le Q'(\bar{u}_k^{(i)}|u_k^{1:i-1}, u_{1:k-1}^{1:N}) < 1$ which is easily satisfied by choosing the low-entropy set $\mathcal{L}_{X_k|X_{1:k-1}}$ properly, we can prove that

$$\sum_{u_k^{(i)}\in\{\bar{u}_k^{(i)}, 1-\bar{u}_k^{(i)}\}} -Q'(u_k^{(i)}|u_k^{1:i-1}, u_{1:k-1}^{1:N}) \log Q'(u_k^{(i)}|u_k^{1:i-1}, u_{1:k-1}^{1:N}) \ge -\log Q'(\bar{u}_k^{(i)}|u_k^{1:i-1}, u_{1:k-1}^{1:N})$$

and hence

$$D_{KL}(Q_{U_k^{(i)}|U_k^{1:i-1}, U_{1:k-1}^{1:N}} \| Q'_{U_k^{(i)}|U_k^{1:i-1}, U_{1:k-1}^{N}}) \le H_P(U_k^{(i)}|U_k^{1:i-1}, U_{1:k-1}^{1:N}).$$

APPENDIX C
FUNCTIONS

At the construction stage, we employed [25, Algorithm A and C] to efficiently calculate the Bhattacharyya parameters. The following Algorithms are key functions at the implementation stage. Algorithm 1 yields $X_k^{1:N}$ given $x_{k-1}^{1:N}$ produced by upper levels of the partition tree as shown in Fig. 4. Due to space limitations, we briefly describe two sub-functions Algorithm 2 and 3 which evolve from [31, recursivelyCalcP(),recursivelyUpdateB()] to efficiently calculate the LRs in equation (18). We keep the notations consistent with Appendix A.

Fig. 7 shows an example of the butterfly circuit to calculate LRs when $N = 8$. We define two properties of each layer, i.e., phase and branch denoted by integers ϕ and ψ, respectively. At layer m, $1 \leq \phi \leq 2^m$ and $0 \leq \psi < 2^{n-m}$. In Fig. 7, we distinguish different phases at each layer by different colors. We have a global array LRReg$[N][n+1]$ indexed by integers $1 \leq i \leq N$ and $0 \leq m \leq n$. Note that for any layer m each integer $1 \leq i \leq 2^n$ has a unique representation as

$$i = \langle \phi, \psi \rangle_m = \phi + 2^m \cdot \psi.$$

Therefore, each element LRReg$[i][m]$ will be uniquely loaded by $L_{2^m}^{(\phi)}$ of phase ϕ and branch ψ in the routine. The other global array of the same size is denoted by UReg$[N][n+1]$ whose elements are single bits. For a generic array A we abbreviate $A[\langle \phi, \psi \rangle_m][m]$ as $A[\langle \phi, \psi \rangle][m]$.

Remark 3: The polar sampler yields samples in a block-by-block fashion rather than one-by-one. What the routines do is to perform exactly $N(\log N+1)$ steps of LR assembling and to yield $X_k^{1:N}$. Despite the if and $else$ statements in Algorithm 1, which conditional branch to go at each iteration of the $for\ loop$ will be fixed given the three index sets. Algorithm 2 and 3 traverse the butterfly circuit and their overall time consumption is only determined by N.

APPENDIX D
UPGRADING AND DEGRADING MERGE

We found it intractable to calculate the Bhattacharyya parameters in (7) and (11) which are then used to define the high and low-entropy sets and the unpolarized set. For each sub-source pair $(U^{(i)}, Y^{1:N} \times U^{1:i-1})$ as in Theorem 3, the alphabet of the side information grows exponentially with the block-lenth N. The upgrading and degrading merge algorithms can approximate the true value of $Z(U^{(i)}|Y^{1:N}, U^{1:i-1})$ by reducing a large alphabet to a manually selected value μ. Moreover, the loss of accuracy can be quantified in terms of entropy. We omit the line-by-line statements of the two algorithms which can be found in [25, Algorithm A and C] but will give how we use them.

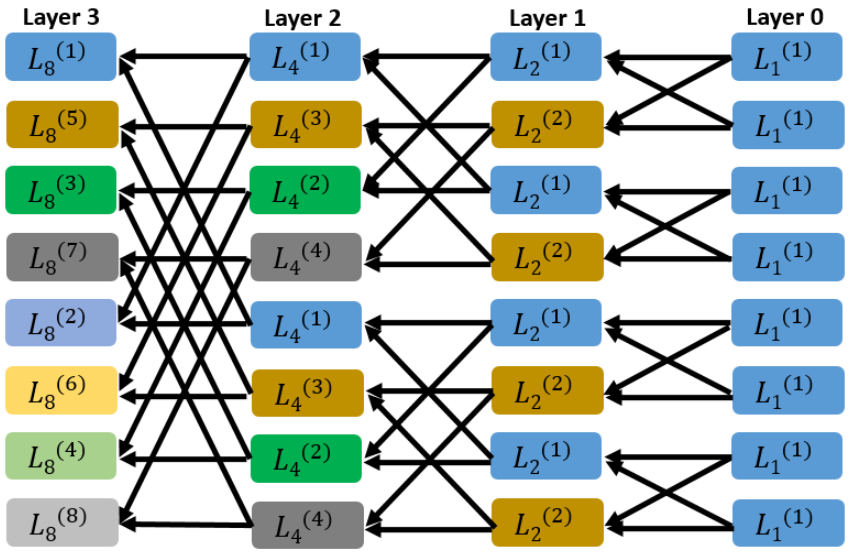

Fig. 7. The butterfly circuit to calculate LR.

Definition 9 (Degraded Channel, [25]): A channel $\mathcal{Q}: \mathcal{X} \to \mathcal{Z}$ is (stochastically) degraded with respect to a channel $\mathcal{W}: \mathcal{X} \to \mathcal{Y}$ if there exists a channel $\mathcal{P}: \mathcal{Y} \to \mathcal{Z}$ such that

$$\mathcal{Q}(z|x) = \sum_{y \in \mathcal{Y}} \mathcal{W}(y|x)\mathcal{P}(z|y)$$

for all $z \in \mathcal{Z}$ and $x \in \mathcal{X}$. We denote by $\mathcal{Q} \preceq \mathcal{W}$ the relation that $\mathcal{Q}$ is degraded with respect to $\mathcal{W}$. Conversely, we denote by $\mathcal{Q}' \succeq \mathcal{W}$ the relation that $\mathcal{Q}'$ is upgraded with respect to $\mathcal{W}$ if there exists a channel $\mathcal{Q}': \mathcal{X} \to \mathcal{Z}'$ and a channel $\mathcal{P}: \mathcal{Z}' \to \mathcal{Y}$ such that

$$\mathcal{W}(y|x) = \sum_{z' \in \mathcal{Z}'} \mathcal{Q}'(z'|x)\mathcal{P}(y|z')$$

for $z' \in \mathcal{Z}$ and $x \in \mathcal{X}$.

Lemma 4 (restatement of lemma 4.7 in [32]): Given the setting as above, we denote by $\mathcal{W}_N^{(i)}$, $\mathcal{Q}_N^{(i)}$ and $\mathcal{Q}_N'^{(i)}$ for $i \in [1, N]$ the sub-channels obtained by Arıkan transformation. If $\mathcal{Q} \preceq \mathcal{W} \preceq \mathcal{Q}'$ for all i, then $\mathcal{Q}_N'^{(i)} \succeq \mathcal{W}_N^{(i)} \succeq \mathcal{Q}_N^{(i)}$.

In order to reduce the complexity of calculating $Z(U^{(i)}|Y^{1:N}, U^{1:i-1})$, we construct the degraded channels (w.p. upgraded channels) with a smaller alphabet than $\mathcal{W}_N^{(i)}$ by degrading merge (w.p. upgrading merge) and obtain the approximation $Z(\mathcal{Q}_N^{(i)})$ (w.p. $Z(\mathcal{Q}_N'^{(i)})$). The following lemma helps illustrate how this approximation will affect the accuracy and the security of the distribution yielded by polar sampling.

Lemma 5 ([25]): Let $\mathcal{W}: \mathcal{X} \to \mathcal{Y}$ be a BMS channel and suppose that $\mathcal{Q}: \mathcal{X} \to \mathcal{Z}$ is degraded with respect to $\mathcal{W}$. Then $Z(\mathcal{Q}) \geq Z(\mathcal{W})$. The inequality will reverse if we replace "degraded" by "upgraded".

input : $L_1^{1:N}$, HighEntropySet, LowEntropySet, (global:LRReg, URegister)

output: $X_k^{1:N}$

LRReg [:][0]=$L_1^{1:N}$;
for $i \leftarrow 1$ **to** N **do**
    LRReg $\leftarrow$ `CalcLR(n,i);`
    if *index* $i \in$ HighEntropySet **then**
        URegister$[i][n] \leftarrow$`randomBin(); // equation (27).`
    end
    else if *index* $i \in$ LowEntropySet **then**
        URegister$[i][n] =$ LRReg$[i][n] < 1$; `// equation (27).`
    end
    else index $i \in$ Non-polarizedSet
        URegister$[i][n] =$`Uniform()` $< 1/(1 +$ LRReg$[i][n])$; `// Uniform() produces real` $y \in (0, 1]$ `uniformly at random; equation (28).`
    end
    URegister $\leftarrow$ `CalcBit(n,i);`
end
return $X_k^{1:N} =$ URegister$[:][0]$

Algorithm 1: Polar sampler for any one level of the partition tree.

Since lemma 4 indicates that Arıkan's transformation preserves the degradation and upgradation relation, it is implied by lemma 5 that $Z(\mathcal{Q}'^{(i)}_N) \leq Z(\mathcal{W}^{(i)}_N) \leq Z(\mathcal{Q}^{(i)}_N)$. Suppose we selected n and β and $\alpha = 2^{-N^\beta}$ appropriately according to a target security level λ. In order to find out the high and low-entropy sets, one needs to compare the following approaches.

- Let $\mathcal{H} = \{i \in N : Z(\mathcal{Q}^{(i)}_N) \in (1-\alpha, 1]\}$ be the high-entropy set and $\mathcal{L} = \{i \in N : Z(\mathcal{Q}^{(i)}_N) \in [0, \alpha)\}$ be the low-entropy set. It can be observed from equation (36) that the accuracy of the resulting distribution will lose a little bit for the high-entropy indexes because $Z(\mathcal{W}^{(i)}_N) \leq Z(\mathcal{Q}^{(i)}_N)$ for $i \in \mathcal{H}$. On the contrary, the accuracy will benefit by the low-entropy indexes according to equation (37).
- If we define $\mathcal{H}$ and $\mathcal{L}$ based exclusively on $Z(\mathcal{Q}'^{(i)}_N)$, the effect on the accuracy for high and low-entropy indexes will reverse.
- If we regard $\mathcal{H} = \{i \in N : Z(\mathcal{Q}'^{(i)}_N) \in (1-\alpha, 1]\}$ as the high-entropy set and regard $\mathcal{L} = \{i \in N : Z(\mathcal{Q}^{(i)}_N) \in [0, \alpha)\}$ as the low-entropy set, it can be guaranteed that the target accuracy and security

input : m, ϕ

output: updated LRReg

if $m = 0$ **then return**;
set $\kappa \leftarrow \lceil \phi/2 \rceil$;
if $\phi \mod 2 = 1$ **then** `CalcLR` $(m-1, \kappa)$;
for $\psi = 0, \cdots, 2^{n-m} - 1$ **do**
    if $\phi \mod 2 = 1$ **then** LRReg $[\langle \phi, \psi \rangle][m] \xleftarrow{\text{equation(39)}}$
    (LRReg$[\langle \kappa, 2\psi \rangle][m-1]$, LRReg$[\langle \kappa, 2\psi+1 \rangle][m-1]$);
    else temp=UReg $[\langle \phi - 1, \psi \rangle][m]$; LRReg $[\langle \phi, \psi \rangle][m] \xleftarrow{\text{equation(40)}}$
    (LRReg$[\langle \kappa, 2\psi \rangle][m-1]$, LRReg$[\langle \kappa, 2\psi+1 \rangle][m-1]$);
end

Algorithm 2: The CalLR( ) function.

input : m, ϕ

output: updated UReg

if $\phi \mod 2 = 1$ **then return**;
set $\kappa \leftarrow \lceil \phi/2 \rceil$;
for $\psi = 0, \cdots, 2^{n-m} - 1$ **do**
    UReg $[\langle \kappa, 2\psi \rangle][m-1] \leftarrow$ UReg$[\langle \phi - 1, \psi \rangle][m] \oplus$ UReg$[\langle \phi, \psi \rangle][m]$;
    UReg $[\langle \kappa, 2\psi+1 \rangle][m-1] \leftarrow$ UReg$[\langle \phi, \psi \rangle][m]$;
end
if $\kappa \mod 2 = 0$ **then** `CalcBit` $(m-1, \kappa)$;

Algorithm 3: The CalBit( ) function.

level is still achievable because of the conservative choices of $\mathcal{H}$ and $\mathcal{L}$.

To avoid the unexpected accuracy and security loss and to make our parameter selection self-consistent, we adopt approach 3 in this work. Although to run both degrading and upgrading merge is time-consuming, it is reasonable and practical as long as these operations are done offline. How to quantify the minor inaccuracy introduced by the merge algorithms deserves more efforts and this is left to future work.

REFERENCES

[1] O. Regev, "On lattices, learning with errors, random linear codes, and cryptography," in *Proceedings of the Thirty-seventh Annual ACM Symposium on Theory of Computing*, ser. STOC '05. New York, NY, USA: ACM, 2005, pp. 84–93.

[2] V. Lyubashevsky, C. Peikert, and O. Regev, "On ideal lattices and learning with errors over rings," in *Annual International Conference on the Theory and Applications of Cryptographic Techniques*. Springer, 2010, pp. 1–23.

[3] D. Micciancio and O. Regev, "Worst-case to average-case reductions based on Gaussian measures," *SIAM Journal on Computing*, vol. 37, no. 1, pp. 267–302, 2007.

[4] D. Micciancio and C. Peikert, "Hardness of SIS and LWE with small parameters," in *Advances in Cryptology–CRYPTO 2013*. Springer, 2013, pp. 21–39.

[5] N. C. Dwarakanath and S. D. Galbraith, "Sampling from discrete Gaussians for lattice-based cryptography on a constrained device," *Applicable Algebra in Engineering, Communication and Computing*, vol. 25, no. 3, pp. 159–180, 2014.

[6] T. Pöppelmann, L. Ducas, and T. Güneysu, "Enhanced lattice-based signatures on reconfigurable hardware," in *International Workshop on Cryptographic Hardware and Embedded Systems*. Springer, 2014, pp. 353–370.

[7] T. Prest, "Gaussian sampling in lattice-based cryptography," Ph.D. dissertation, École Normale Supérieure, 2015.

[8] ——, "Sharper bounds in lattice-based cryptography using the Rényi divergence," in *International Conference on the Theory and Application of Cryptology and Information Security*. Springer, 2017, pp. 347–374.

[9] S. Bai, T. Lepoint, A. Roux-Langlois, A. Sakzad, D. Stehlé, and R. Steinfeld, "Improved security proofs in lattice-based cryptography: Using the Rényi divergence rather than the statistical distance," *Journal of Cryptology*, vol. 31, no. 2, pp. 610–640, 2018.

[10] L. Ducas, A. Durmus, T. Lepoint, and V. Lyubashevsky, "Lattice signatures and bimodal Gaussians," in *Advances in Cryptology – CRYPTO 2013*, R. Canetti and J. A. Garay, Eds. Berlin, Heidelberg: Springer Berlin Heidelberg, 2013, pp. 40–56.

[11] L. Devroye, "Sample-based non-uniform random variate generation," in *Proceedings of the 18th conference on Winter simulation*. ACM, 1986, pp. 260–265.

[12] D. Knuth, "The complexity of nonuniform random number generation," *Algorithm and Complexity, New Directions and Results*, pp. 357–428, 1976.

[13] G. Marsaglia, W. W. Tsang *et al.*, "The Ziggurat method for generating random variables," *Journal of Statistical Software*, vol. 5, no. 8, pp. 1–7, 2000.

[14] C. Peikert, "An efficient and parallel Gaussian sampler for lattices," in *Annual Cryptology Conference*. Springer, 2010, pp. 80–97.

[15] A. Karmakar, S. S. Roy, O. Reparaz, F. Vercauteren, and I. Verbauwhede, "Constant-time discrete Gaussian sampling," *IEEE Transactions on Computers*, vol. 67, no. 11, pp. 1561–1571, 2018.

[16] A. Hülsing, T. Lange, and K. Smeets, "Rounded Gaussians – fast and secure constant-time sampling for lattice-based crypto," Cryptology ePrint Archive, Report 2017/1025, 2017.

[17] G. E. P. Box and M. E. Muller, "A note on the generation of random normal deviates," *Ann. Math. Statist.*, vol. 29, no. 2, pp. 610–611, 06 1958.

[18] D. Micciancio and M. Walter, "Gaussian sampling over the integers: Efficient, generic, constant-time," in *Annual International Cryptology Conference*. Springer, 2017, pp. 455–485.

[19] R. K. Zhao, R. Steinfeld, and A. Sakzad, "FACCT: Fast, Compact, and Constant-Time Discrete Gaussian Sampler over Integers," Cryptology ePrint Archive, Report 2018/1234, 2018.

[20] M.-J. O. Saarinen, "Arithmetic coding and blinding countermeasures for lattice signatures," *Journal of Cryptographic Engineering*, vol. 8, no. 1, pp. 71–84, Apr 2018.

[21] E. Arikan, "Channel polarization: A method for constructing capacity-achieving codes for symmetric binary-input memoryless channels," *IEEE Transactions on Information Theory*, vol. 55, no. 7, pp. 3051–3073, 2009.

[22] E. Arikan, "Source polarization," in *2010 IEEE International Symposium on Information Theory*, June 2010, pp. 899–903.

[23] T. M. Cover and J. A. Thomas, *Elements of Information Theory*. John Wiley & Sons, 2012.

[24] J. Honda and H. Yamamoto, "Polar coding without alphabet extension for asymmetric models," *IEEE Transactions on Information Theory*, vol. 59, no. 12, pp. 7829–7838, 2013.

[25] I. Tal and A. Vardy, "How to construct polar codes," *IEEE Transactions on Information Theory*, vol. 59, no. 10, pp. 6562–6582, 2013.

[26] R. Mori and T. Tanaka, "Performance of polar codes with the construction using density evolution," *IEEE Communications Letters*, vol. 13, no. 7, 2009.

[27] L. Liu, Y. Yan, C. Ling, and X. Wu, "Construction of capacity-achieving lattice codes: Polar lattices," *IEEE Transactions on Communications*, vol. 67, no. 2, pp. 915–928, 2019.

[28] C. Gentry, C. Peikert, and V. Vaikuntanathan, "Trapdoors for hard lattices and new cryptographic constructions," in *Proceedings of the fortieth annual ACM symposium on Theory of computing*. ACM, 2008, pp. 197–206.

[29] J. Howe, A. Khalid, C. Rafferty, F. Regazzoni, and M. O'Neill, "On practical discrete gaussian samplers for lattice-based cryptography," *IEEE Transactions on Computers*, vol. 67, no. 3, pp. 322–334, 2016.

[30] T. Pöppelmann, L. Ducas, and T. Güneysu, "Enhanced lattice-based signatures on reconfigurable hardware," in *Cryptographic Hardware and Embedded Systems – CHES 2014*, L. Batina and M. Robshaw, Eds. Berlin, Heidelberg: Springer Berlin Heidelberg, 2014, pp. 353–370.

[31] I. Tal and A. Vardy, "List decoding of polar codes," *IEEE Transactions on Information Theory*, vol. 61, no. 5, pp. 2213–2226, 2015.

[32] S. B. Korada, "Polar codes for channel and source coding," EPFL, Tech. Rep., 2009.